Nonlinear optical interactions of wave packets in photonic crystals: Hamiltonian dynamics of effective fields

S. N. Volkov and J. E. Sipe
Department of Physics, University of Toronto, 60 St. George Street, Toronto, Ontario, Canada M5S 1A7
(Received 2 April 2004; published 23 December 2004)

We develop an effective-field formalism that is suitable for describing nonlinear interactions of multiple wave packets in photonic crystals of arbitrary dimensionality. The theory is valid for "high-contrast" variations of the refractive index in the photonic crystal, provided dispersion and absorption effects can be neglected; it is based on a Hamiltonian formulation of the underlying Maxwell equations. We show that the dynamical equations for the effective fields are similar to those commonly used in nonlinear optics of homogeneous media, but with coefficients determined from the photonic band structure. We can introduce an effective energy density and an effective Poynting vector, expressed in terms of the effective fields, that satisfy a continuity equation. We illustrate our approach with a solution of the problem of degenerate optical parametric amplification in the undepleted pump approximation, and by considering the linear electro-optic effect as a quadratic nonlinear optical process.

DOI: 10.1103/PhysRevE.70.066621 PACS number(s): 42.70.Qs, 42.65.−k, 03.50.De

I. INTRODUCTION

Photonic crystals [1,2] provide new opportunities for enhancing and controlling nonlinear optical processes, such as second-harmonic generation, optical parametric amplification, and self- and cross-phase modulation. In the past few decades different theoretical approaches have been developed for describing nonlinear processes in "low contrast" periodic materials [3], where there is only a small variation in the linear refractive index, usually with a focus on one-dimensional periodic waveguide structures. These traditional approaches are not appropriate for the kind of "high-contrast" variations in the linear optical properties that are typical of two- and three-dimensional photonic crystals. A straightforward multiple-scales analysis based on slowly-varying amplitudes introduced for the different Bloch functions can be applied to such problems, but it is often cumbersome [4]. Recently, an effective-fields formalism has been proposed, based on a Hamiltonian formulation of the underlying dynamics of the electromagnetic field [5,6]. This approach is applicable to high-contrast structures, and yet less awkward than the earlier multiple-scales analyses. We demonstrate that an extension of this effective-fields formalism allows us to describe different wave mixing processes in high-contrast photonic crystals in a convenient and intuitive way.

In the effective-fields formalism, wave packets in a photonic crystal are comprised of Bloch functions in the same photonic band with close wave-vector indices; the contributions of the different Bloch functions to a wave packet are described by a slowly varying function of the wave-vector index. The effective field is the Fourier transform of this wave-vector function, which is a slowly varying function of the spatial coordinates. The effective fields give an "averaged" description for the electromagnetic field in a periodic medium; in terms of them expressions for the average energy density and Poynting vector can be given. In this paper, we show that the dynamical equations for the effective fields are similar to those commonly used in nonlinear optics of homogeneous media, but with coefficients determined from the photonic band structure. In contrast, if one introduces wave packets in photonic crystals *via* a slowly varying envelope function that multiplies a Bloch-function "carrier" wave, the corresponding dynamical equations [4] are much harder to obtain [7].

In Sec. II we introduce the basic equations and the notation that we will use further in the article. We assume that the dielectric media comprising the photonic crystal are nondispersive, nonmagnetic and without absorption. When writing down the dynamical equations, we use a Hamiltonian approach that not only simplifies our formulas, but allows us to quantize the problem easily, and to find conserved quantities and investigate their relation to symmetries. In the constitutive relations and dynamical equations for the electromagnetic field we treat the electric displacement field $\boldsymbol{D}(\boldsymbol{r},t)$ and the magnetic field $\boldsymbol{B}(\boldsymbol{r},t)$ as our fundamental fields, since their exact transversality can be automatically guaranteed. The strength of this choice of the fundamental fields was first pointed out by Born and Infeld [8] and discussed in more detail in [9]; a helpful review of different approaches to canonical quantization in light propagation problems can be found in [10]. We introduce Bloch eigenmodes of the photonic crystal [1], and write down the dynamical equations for the coefficients of the Bloch-mode expansion of the electric field $\boldsymbol{D}(\boldsymbol{r},t)$. For simplicity, we limit ourselves to considering only the quadratic optical nonlinearity, and we use negative band indices to make our notation suitable for simultaneous description of the field-expansion coefficients and their complex- (or Hermitian-) conjugated counterparts.

Section III, where we present a step-by-step introduction of the effective-fields formalism for multiple wave-packets interaction, contains the main result of our article. We start with defining wave packets for a convenient description of nonlinear wave-mixing processes and deriving the corresponding dynamical equations. We have to generalize the definition of the wave packet used in [6] to allow for mul-

tiple wave packets in the same photonic band; it leads to a modified Poisson bracket that is no longer canonical, but still is almost as convenient to use. Then we introduce the effective fields and derive the dynamical equation for them. We also obtain a continuity equation for the effective energy density and the effective Poynting vector, which connects the effective fields with wave-packet intensities.

To demonstrate the approach in some detail, in Sec. IV we apply our formalism to solving two simple problems of nonlinear optical interaction in a photonic crystal with a nonvanishing quadratic susceptibility. First, we consider degenerate optical parametric amplification in the simplest case of plane-wave geometry and undepleted pump approximation. Not unexpectedly, the lowest order approximation of our treatment agrees with the result of a more *ad hoc* perturbation theory. Next, we show that the effective-fields formalism is also applicable for describing the linear electro-optic effect, that we treated as a second-order nonlinear process, with one of the interacting wave packets being the constant electric field applied to the photonic crystal. The advantage of such a description over a simple modification of the refractive index according to the constant electric field and subsequent finding of "shifted" Bloch functions is that we can also describe the effect with the electric field being nonuniform (slowly varying) in space (or time). We present our conclusions in Sec. V.

II. BASIC EQUATIONS

A. Constitutive relations

The constitutive relations in a nonmagnetic medium are usually written as

$$\boldsymbol{D}(\boldsymbol{r},t) = \varepsilon_0 \boldsymbol{E}(\boldsymbol{r},t) + \boldsymbol{P}(\boldsymbol{r},t), \tag{1}$$

$$\boldsymbol{B}(\boldsymbol{r},t) = \mu_0 \boldsymbol{H}(\boldsymbol{r},t), \tag{2}$$

where the polarization of the medium $\boldsymbol{P}(\boldsymbol{r},t)$ depends on the electric field $\boldsymbol{E}(\boldsymbol{r},t)$, in general in a nonlocal way. Contrary to this approach, we use $\boldsymbol{D}(\boldsymbol{r},t)$ and $\boldsymbol{B}(\boldsymbol{r},t)$, rather than $\boldsymbol{E}(\boldsymbol{r},t)$ and $\boldsymbol{H}(\boldsymbol{r},t)$, as independent dynamical variables [8]. Thus we reverse the constitutive relations to express $\boldsymbol{E}(\boldsymbol{r},t)$ and $\boldsymbol{P}(\boldsymbol{r},t)$ in terms of $\boldsymbol{D}(\boldsymbol{r},t)$ and $\boldsymbol{H}(\boldsymbol{r},t)$ in terms of $\boldsymbol{B}(\boldsymbol{r},t)$; the latter is, of course, trivial. We further assume that the polarization $\boldsymbol{P}(\boldsymbol{r},t)$ only depends locally on $\boldsymbol{D}(\boldsymbol{r},t)$, in both space and time. This implies that we are far from any resonant frequencies of the material, and that any absorption is negligible. Further assuming that the linear optical response is isotropic, we can separate $\boldsymbol{P}(\boldsymbol{r},t)$ into linear and nonlinear parts as

$$\boldsymbol{P}(\boldsymbol{r},t) = \frac{n^2(\boldsymbol{r})-1}{n^2(\boldsymbol{r})}\boldsymbol{D}(\boldsymbol{r},t) + \boldsymbol{P}_{\mathrm{NL}}(\boldsymbol{r},t), \tag{3}$$

so in the linear limit the commonly used relation between $\boldsymbol{D}(\boldsymbol{r},t)$ and $\boldsymbol{E}(\boldsymbol{r},t)$ becomes simply

$$\boldsymbol{D}(\boldsymbol{r},t) = \varepsilon_0 n^2(\boldsymbol{r})\boldsymbol{E}(\boldsymbol{r},t), \tag{4}$$

where $n(\boldsymbol{r})$ is then identified as the refractive index, which we take to be real. The nonlinear polarization is represented as a power series in $\boldsymbol{D}(\boldsymbol{r},t)$:

$$P^i_{\mathrm{NL}}(\boldsymbol{r},t) = \Gamma_2^{ijl}(\boldsymbol{r})D^j(\boldsymbol{r},t)D^l(\boldsymbol{r},t) + \Gamma_3^{ijlm}(\boldsymbol{r})D^j(\boldsymbol{r},t)D^l(\boldsymbol{r},t)D^m(\boldsymbol{r},t) + \cdots. \tag{5}$$

This tensor expression implies summation over the repeating Cartesian indices, that we will generally denote as i,j,l,m, writing them as superscripts. The nonlinear "$\boldsymbol{D}$-susceptibilities" are symmetric with respect to the permutation of any of their Cartesian indices. This "full permutation symmetry" [12,13] follows because of the non-resonant character of the nonlinear optical interaction.

It is customary to express $\boldsymbol{P}(\boldsymbol{r},t)$ in terms of $\boldsymbol{E}(\boldsymbol{r},t)$ rather than $\boldsymbol{D}(\boldsymbol{r},t)$ according to the following formula:

$$P^i(\boldsymbol{r},t) = \varepsilon_0\{[n^2(\boldsymbol{r})-1]E^i(\boldsymbol{r},t) + \chi^{(2)}_{ijl}(\boldsymbol{r})E^j(\boldsymbol{r},t)E^l(\boldsymbol{r},t) + \chi^{(3)}_{ijlm}(\boldsymbol{r})E^j(\boldsymbol{r},t)E^l(\boldsymbol{r},t)E^m(\boldsymbol{r},t) + \cdots\}. \tag{6}$$

The relations between the susceptibilities $\overleftrightarrow{\Gamma}_n(\boldsymbol{r})$ and the "traditional" susceptibilities $\overleftrightarrow{\chi}^{(n)}(\boldsymbol{r})$ are obtained by substituting Eqs. (1) and (6) into Eqs. (3) and (5) and comparing the coefficients of different powers of $\boldsymbol{E}$ in the resulting expression with those in Eq. (6). This gives us the following relations:

$$\Gamma_2^{ijl}(\boldsymbol{r}) = \frac{\chi^{(2)}_{ijl}(\boldsymbol{r})}{\varepsilon_0 n^6(\boldsymbol{r})}, \tag{7}$$

$$\Gamma_3^{ijlm}(\boldsymbol{r}) = \frac{1}{\varepsilon_0^2 n^8(\boldsymbol{r})}\left[\chi^{(3)}_{ijlm}(\boldsymbol{r}) - \frac{2}{n^2(\boldsymbol{r})}\chi^{(2)}_{ijq}(\boldsymbol{r})\chi^{(2)}_{qlm}(\boldsymbol{r})\right]. \tag{8}$$

B. Hamiltonian formalism for the electromagnetic field

A Hamiltonian that gives the dynamical equations for the electromagnetic field is

$$\mathcal{H} = \mathcal{H}_0 + \mathcal{H}_{\mathrm{NL}}, \tag{9}$$

where $\mathcal{H}_0$ describes the linear optical response,

$$\mathcal{H}_0 = \int d\boldsymbol{r}\frac{\boldsymbol{D}(\boldsymbol{r},t)\cdot\boldsymbol{D}(\boldsymbol{r},t)}{2\varepsilon_0 n^2(\boldsymbol{r})} + \int d\boldsymbol{r}\frac{\boldsymbol{B}(\boldsymbol{r},t)\cdot\boldsymbol{B}(\boldsymbol{r},t)}{2\mu_0}, \tag{10}$$

and $\mathcal{H}_{\mathrm{NL}}$ describes nonlinear effects,

$$\mathcal{H}_{\mathrm{NL}} = -\frac{1}{3\varepsilon_0}\int d\boldsymbol{r}\Gamma_2^{ijl}(\boldsymbol{r})D^i(\boldsymbol{r},t)D^j(\boldsymbol{r},t)D^l(\boldsymbol{r},t) - \frac{1}{4\varepsilon_0}\int d\boldsymbol{r}\Gamma_3^{ijlm}(\boldsymbol{r})D^i(\boldsymbol{r},t)D^j(\boldsymbol{r},t)D^l(\boldsymbol{r},t)D^m(\boldsymbol{r},t) + \cdots. \tag{11}$$

The Hamiltonian $\mathcal{H}$ is equal to the total energy of the electromagnetic field.

The fields $\boldsymbol{D}(\boldsymbol{r},t)$ and $\boldsymbol{B}(\boldsymbol{r},t)$ are transverse even in the presence of nonlinear interactions, which allows us to leave out all unphysical solutions by restricting our dynamical space to transverse functions. This ease in dealing with the transversality conditions on $\boldsymbol{D}(\boldsymbol{r},t)$ and $\boldsymbol{B}(\boldsymbol{r},t)$ is the reason for our somewhat unusual choice of them as our field variables.

When used with the Hamiltonian (9), the Poisson brackets for $\boldsymbol{D}(\boldsymbol{r},t)$ and $\boldsymbol{B}(\boldsymbol{r},t)$ that give the correct dynamical equations are [8]

$$[D^i(\boldsymbol{r},t),D^j(\boldsymbol{r}',t)]=0, \tag{12}$$

$$[B^i(\boldsymbol{r},t),B^j(\boldsymbol{r}',t)]=0, \tag{13}$$

$$[D^i(\boldsymbol{r},t),B^j(\boldsymbol{r}',t)]=-i\hbar\epsilon^{ijl}\frac{\partial}{\partial r^l}\delta(\boldsymbol{r}-\boldsymbol{r}'), \tag{14}$$

where ϵ^{ijl} is the unit antisymmetric Levi-Civita tensor. Here and below we use a notation for the Poisson bracket,

$$\frac{1}{i\hbar}[\ldots,\ldots]\equiv\{\ldots,\ldots\}, \tag{15}$$

that emphasizes the similarity of the classical equations to their quantum counterparts. With the choice of Eqs. (12)–(14), the usual Hamilton's equations,

$$\frac{\partial}{\partial t}\boldsymbol{D}(\boldsymbol{r},t)=\frac{1}{i\hbar}[\boldsymbol{D}(\boldsymbol{r},t),\mathcal{H}], \tag{16}$$

$$\frac{\partial}{\partial t}\boldsymbol{B}(\boldsymbol{r},t)=\frac{1}{i\hbar}[\boldsymbol{B}(\boldsymbol{r},t),\mathcal{H}], \tag{17}$$

lead to the dynamical equations for $\boldsymbol{D}(\boldsymbol{r},t)$ and $\boldsymbol{B}(\boldsymbol{r},t)$, which are simply the two vector Maxwell equations in a dielectric medium.

C. Bloch modes and their properties

In a photonic crystal all material properties are periodic functions of $\boldsymbol{r}$; for example, $n(\boldsymbol{r})=n(\boldsymbol{r}+\boldsymbol{R})$, $\Gamma_2^{ijl}(\boldsymbol{r})=\Gamma_2^{ijl}(\boldsymbol{r}+\boldsymbol{R})$, etc., where $\boldsymbol{R}$ is an arbitrary lattice vector of the photonic crystal. In the following, we consider 3D photonic crystals, but, unless otherwise noted, all formulas are quite general and applicable with minor obvious modifications to 2D and 1D photonic crystals; the notational differences have been discussed earlier [6].

The linearized dynamical equations for $\boldsymbol{D}(\boldsymbol{r},t)$ and $\boldsymbol{B}(\boldsymbol{r},t)$ are obtained by neglecting the nonlinear polarization of the medium $\boldsymbol{P}_{\mathrm{NL}}(\boldsymbol{r},t)$ in the two Maxwell equations written in terms of $\boldsymbol{D}(\boldsymbol{r},t)$ and $\boldsymbol{B}(\boldsymbol{r},t)$:

$$\frac{\partial}{\partial t}\boldsymbol{D}(\boldsymbol{r},t)=\frac{1}{\mu_0}\boldsymbol{\nabla}\times\boldsymbol{B}(\boldsymbol{r},t), \tag{18}$$

$$\frac{\partial}{\partial t}\boldsymbol{B}(\boldsymbol{r},t)=-\frac{1}{\varepsilon_0}\boldsymbol{\nabla}\times\left(\frac{\boldsymbol{D}(\boldsymbol{r},t)}{n^2(\boldsymbol{r})}\right). \tag{19}$$

Their stationary solutions take the form

$$\boldsymbol{D}(\boldsymbol{r},t)=\boldsymbol{D}_{n\boldsymbol{k}}(\boldsymbol{r})\exp(-i\omega_{n\boldsymbol{k}}t), \tag{20}$$

$$\boldsymbol{B}(\boldsymbol{r},t)=\boldsymbol{B}_{n\boldsymbol{k}}(\boldsymbol{r})\exp(-i\omega_{n\boldsymbol{k}}t), \tag{21}$$

where $\omega_{n\boldsymbol{k}}$ is the eigenfrequency corresponding to the pair of spatial field eigenmodes $(\boldsymbol{D}_{n\boldsymbol{k}}(\boldsymbol{r}),\boldsymbol{B}_{n\boldsymbol{k}}(\boldsymbol{r}))$. Physical fields are always real, and they contain these eigenmodes in complex-conjugated pairs. For the moment we restrict ourselves to positive $\omega_{n\boldsymbol{k}}$, and take the photonic band index n to run only over positive integers; we will generalize this below.

According to Bloch's theorem, $\boldsymbol{D}_{n\boldsymbol{k}}(\boldsymbol{r})$ and $\boldsymbol{B}_{n\boldsymbol{k}}(\boldsymbol{r})$ (often referred to as Bloch functions or Bloch modes) can be written as

$$\boldsymbol{D}_{n\boldsymbol{k}}(\boldsymbol{r})=\frac{1}{\sqrt{8\pi^3}}\boldsymbol{d}_{n\boldsymbol{k}}(\boldsymbol{r})\exp(i\boldsymbol{k}\cdot\boldsymbol{r}), \tag{22}$$

$$\boldsymbol{B}_{n\boldsymbol{k}}(\boldsymbol{r})=\frac{1}{\sqrt{8\pi^3}}\boldsymbol{b}_{n\boldsymbol{k}}(\boldsymbol{r})\exp(i\boldsymbol{k}\cdot\boldsymbol{r}), \tag{23}$$

where $\boldsymbol{d}_{n\boldsymbol{k}}(\boldsymbol{r})$ and $\boldsymbol{b}_{n\boldsymbol{k}}(\boldsymbol{r})$ are periodic functions of $\boldsymbol{r}$,

$$\boldsymbol{d}_{n\boldsymbol{k}}(\boldsymbol{r})=\boldsymbol{d}_{n\boldsymbol{k}}(\boldsymbol{r}+\boldsymbol{R}), \tag{24}$$

$$\boldsymbol{b}_{n\boldsymbol{k}}(\boldsymbol{r})=\boldsymbol{b}_{n\boldsymbol{k}}(\boldsymbol{r}+\boldsymbol{R}), \tag{25}$$

with $\boldsymbol{R}$ an arbitrary lattice vector of the photonic crystal. The factor of $1/\sqrt{8\pi^3}$ is introduced for further convenience; it is specific to the 3D case, and different factors would be more useful in 1D and 2D problems (see [6]); $\boldsymbol{k}$ is a wave-vector index that varies continuously and is restricted to the first Brillouin zone, which we denote as Ω_{B}. Subsequently, all $\boldsymbol{k}$-dependent quantities are only defined for $\boldsymbol{k}\in\Omega_{\mathrm{B}}$ unless otherwise noted.

Finding the modes $\boldsymbol{D}_{n\boldsymbol{k}}(\boldsymbol{r})$ and $\boldsymbol{B}_{n\boldsymbol{k}}(\boldsymbol{r})$ is straightforward and easily done numerically using established algorithms; programs implementing them are readily available [11]. Note that the $\boldsymbol{D}_{n\boldsymbol{k}}(\boldsymbol{r})$ modes are connected to the more commonly used $\boldsymbol{E}_{n\boldsymbol{k}}(\boldsymbol{r})$ modes by a simple relation:

$$\varepsilon_0 n^2(\boldsymbol{r})\boldsymbol{E}_{n\boldsymbol{k}}(\boldsymbol{r})=\boldsymbol{D}_{n\boldsymbol{k}}(\boldsymbol{r}). \tag{26}$$

All the $\boldsymbol{D}_{n\boldsymbol{k}}(\boldsymbol{r})$ and $\boldsymbol{B}_{n\boldsymbol{k}}(\boldsymbol{r})$ are naturally transverse, so they form a convenient basis set for the transverse fields $\boldsymbol{D}(\boldsymbol{r},t)$ and $\boldsymbol{B}(\boldsymbol{r},t)$.

The linearized dynamical field equations (18) and (19) possess important symmetries that follow from the time-reversal symmetry of the Maxwell equations. In particular,

$$\omega_{n(-\boldsymbol{k})}=\omega_{n\boldsymbol{k}}, \tag{27}$$

which implies that the first Brillouin zone Ω_{B} has center-of-inversion symmetry, whether the photonic crystal itself does or does not have that symmetry. It also follows that we can choose the eigensolutions [6] such that they satisfy

$$\boldsymbol{D}_{n(-\boldsymbol{k})}(\boldsymbol{r})=\boldsymbol{D}_{n\boldsymbol{k}}^*(\boldsymbol{r}), \tag{28}$$

$$\boldsymbol{B}_{n(-\boldsymbol{k})}(\boldsymbol{r})=-\boldsymbol{B}_{n\boldsymbol{k}}^*(\boldsymbol{r}). \tag{29}$$

Corresponding symmetries apply to $\boldsymbol{d}_{n\boldsymbol{k}}(\boldsymbol{r})$ and $\boldsymbol{b}_{n\boldsymbol{k}}(\boldsymbol{r})$. Of course, additional mode symmetries may arise due to rotational and reflection symmetries of the photonic-crystal lattice.

The magnitudes of the spatial field eigenmodes $\boldsymbol{D}_{n\boldsymbol{k}}(\boldsymbol{r})$ and $\boldsymbol{B}_{n\boldsymbol{k}}(\boldsymbol{r})$ can be chosen [6] so that

$$\int d\boldsymbol{r}\frac{\boldsymbol{D}^{*}_{n\boldsymbol{k}}(\boldsymbol{r})\cdot\boldsymbol{D}_{n'\boldsymbol{k}'}(\boldsymbol{r})}{\varepsilon_0 n^2(\boldsymbol{r})}=\frac{\hbar\omega_{n\boldsymbol{k}}}{2}\delta_{nn'}\delta(\boldsymbol{k}-\boldsymbol{k}'),\qquad(30)$$

$$\int d\boldsymbol{r}\frac{\boldsymbol{B}^{*}_{n\boldsymbol{k}}(\boldsymbol{r})\cdot\boldsymbol{B}_{n'\boldsymbol{k}'}(\boldsymbol{r})}{\mu_0}=\frac{\hbar\omega_{n\boldsymbol{k}}}{2}\delta_{nn'}\delta(\boldsymbol{k}-\boldsymbol{k}'),\qquad(31)$$

where the integrations are performed over an infinite volume and the factors appearing on the right-hand side are set for convenience. We consider the left-hand sides of Eqs. (30) and (31) as the scalar products in the spaces of modes $\boldsymbol{D}_{n\boldsymbol{k}}(\boldsymbol{r})$ and $\boldsymbol{B}_{n\boldsymbol{k}}(\boldsymbol{r})$, respectively. Thus these equations constitute the orthonormality conditions for the modes. The orthogonality of modes corresponding to different frequencies $\omega_{n\boldsymbol{k}}$ follows from the Hermiticity (with respect to the scalar products just defined) of the operators that act on $\boldsymbol{D}_{n\boldsymbol{k}}(\boldsymbol{r})$ and $\boldsymbol{B}_{n\boldsymbol{k}}(\boldsymbol{r})$ in wave equations that can be derived from Eqs. (18) and (19) for each of those fields [6]. Thus it is only degenerate modes that, by the choice of their form, must be explicitly orthogonalized.

We now generalize this notation by introducing a band index n that accepts both positive and negative integer values, so that

$$\omega_{(-n)\boldsymbol{k}}\equiv-\omega_{n(-\boldsymbol{k})}.\qquad(32)$$

The corresponding modes with negative index are defined according to

$$\boldsymbol{D}_{(-n)\boldsymbol{k}}(\boldsymbol{r})\equiv\boldsymbol{D}^{*}_{n(-\boldsymbol{k})}(\boldsymbol{r}),\qquad(33)$$

$$\boldsymbol{B}_{(-n)\boldsymbol{k}}(\boldsymbol{r})\equiv\boldsymbol{B}^{*}_{n(-\boldsymbol{k})}(\boldsymbol{r}),\qquad(34)$$

and it is easy to confirm that these negative-index solutions, when used in Eqs. (20) and (21), also satisfy Eqs. (18) and (19).

These symmetries of the spatial field modes and the introduction of bands with negative indices are illustrated by Fig. 1. The use of these negative-index solutions will considerably simplify our notation below. Taking into account the symmetries expressed by Eqs. (28) and (29) and the definitions of the modes with negative band indices (33) and (34), we conclude that $\boldsymbol{D}_{(-n)\boldsymbol{k}}(\boldsymbol{r})$ is the same as $\boldsymbol{D}_{n\boldsymbol{k}}(\boldsymbol{r})$, and $\boldsymbol{B}_{(-n)\boldsymbol{k}}(\boldsymbol{r})$ is the same as $-\boldsymbol{B}_{n\boldsymbol{k}}(\boldsymbol{r})$, that is, only a half of all $\boldsymbol{D}_{n\boldsymbol{k}}(\boldsymbol{r})$ and a half of all $\boldsymbol{B}_{n\boldsymbol{k}}(\boldsymbol{r})$ are independent. Still, the pairs of modes $(\boldsymbol{D}_{(-n)\boldsymbol{k}}(\boldsymbol{r}),\boldsymbol{B}_{(-n)\boldsymbol{k}}(\boldsymbol{r}))$ and $(\boldsymbol{D}_{n\boldsymbol{k}}(\boldsymbol{r}),\boldsymbol{B}_{n\boldsymbol{k}}(\boldsymbol{r}))$ are different, so we can say that all pairs of spatial field modes are independent, and they satisfy the following generalized orthogonality relation,

$$\int d\boldsymbol{r}\left\{\frac{\boldsymbol{D}^{*}_{n\boldsymbol{k}}(\boldsymbol{r})\cdot\boldsymbol{D}_{n'\boldsymbol{k}'}(\boldsymbol{r})}{\varepsilon_0 n^2(\boldsymbol{r})}+\frac{\boldsymbol{B}^{*}_{n\boldsymbol{k}}(\boldsymbol{r})\cdot\boldsymbol{B}_{n'\boldsymbol{k}'}(\boldsymbol{r})}{\mu_0}\right\}=\hbar|\omega_{n\boldsymbol{k}}|\delta_{nn'}\delta(\boldsymbol{k}-\boldsymbol{k}'),\qquad(35)$$

in which n and n' can accept both positive and negative values. This orthogonality relation for pairs $(\boldsymbol{D}_{n\boldsymbol{k}}(\boldsymbol{r}),\boldsymbol{B}_{n\boldsymbol{k}}(\boldsymbol{r}))$ can be obtained from (and is equivalent to) the two separate orthogonality relations for $\boldsymbol{D}_{n\boldsymbol{k}}(\boldsymbol{r})$ and $\boldsymbol{B}_{n\boldsymbol{k}}(\boldsymbol{r})$, restricted to positive n only.

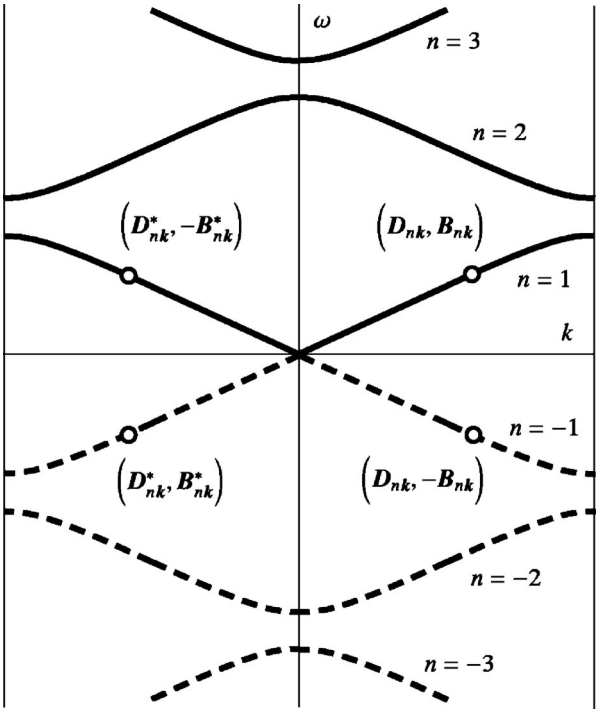

FIG. 1. Symmetries of the spatial field modes $(\boldsymbol{D}_{n\boldsymbol{k}}(\boldsymbol{r}),\boldsymbol{B}_{n\boldsymbol{k}}(\boldsymbol{r}))$, illustrated for a 1D photonic crystal, that originate from the time-reversal symmetry of the Maxwell equations. The negative-index photonic bands (dashed lines) are mirror-symmetric to the positive-index bands (solid lines) with respect to the k axis.

D. Field dynamics in terms of the mode-expansion coefficients

We can expand $\boldsymbol{D}(\boldsymbol{r},t)$ and $\boldsymbol{B}(\boldsymbol{r},t)$ in the positive-index Bloch modes $\boldsymbol{D}_{n\boldsymbol{k}}(\boldsymbol{r})$ and $\boldsymbol{B}_{n\boldsymbol{k}}(\boldsymbol{r})$ [6] according to

$$\boldsymbol{D}(\boldsymbol{r},t)=\sum_{n>0}\int_{\Omega_{\mathrm{B}}}d\boldsymbol{k}[a_{n\boldsymbol{k}}(t)\boldsymbol{D}_{n\boldsymbol{k}}(\boldsymbol{r})+a^{\dagger}_{n\boldsymbol{k}}(t)\boldsymbol{D}^{*}_{n\boldsymbol{k}}(\boldsymbol{r})],\qquad(36)$$

$$\boldsymbol{B}(\boldsymbol{r},t)=\sum_{n>0}\int_{\Omega_{\mathrm{B}}}d\boldsymbol{k}[a_{n\boldsymbol{k}}(t)\boldsymbol{B}_{n\boldsymbol{k}}(\boldsymbol{r})+a^{\dagger}_{n\boldsymbol{k}}(t)\boldsymbol{B}^{*}_{n\boldsymbol{k}}(\boldsymbol{r})],\qquad(37)$$

where in a quantum problem the mode-expansion coefficients $a_{n\boldsymbol{k}}(t)$ and $a^{\dagger}_{n\boldsymbol{k}}(t)$ are the annihilation and creation operators for photons in the band n with the wave vector $\boldsymbol{k}$; in a classical problem they are appropriate combination of the canonical coordinate and momentum associated with each mode. We adopt the quantum notation, in which $a^{\dagger}_{n\boldsymbol{k}}(t)$ is the Hermitian conjugate of $a_{n\boldsymbol{k}}(t)$; in a classical problem we take $a^{\dagger}_{n\boldsymbol{k}}(t)$ to mean $a^{*}_{n\boldsymbol{k}}(t)$.

The Poisson bracket for $a_{n\boldsymbol{k}}(t)$ is obtained from the Poisson brackets for $\boldsymbol{D}(\boldsymbol{r},t)$ and $\boldsymbol{B}(\boldsymbol{r},t)$ (12)–(14) using the completeness of the basis sets formed by the Bloch modes $\boldsymbol{D}_{n\boldsymbol{k}}(\boldsymbol{r})$ and $\boldsymbol{B}_{n\boldsymbol{k}}(\boldsymbol{r})$; we find

$$[a_{n\boldsymbol{k}}(t),a^{\dagger}_{n'\boldsymbol{k}'}(t)]=\delta_{nn'}\delta(\boldsymbol{k}-\boldsymbol{k}')\qquad(38)$$

(see also [6]). This is the usual Poisson bracket for these variables in a classical problem, or the commutation relation for these operators in a quantum problem.

It is convenient to introduce dynamical variables $c_{n\boldsymbol{k}}(t)$ that give us simpler mode expansion formulas for the fields. We define the $c_{n\boldsymbol{k}}(t)$ for both positive and negative band indices n,

$$c_{n\boldsymbol{k}}(t) \equiv \begin{cases} a_{n\boldsymbol{k}}(t), & \text{for } n > 0, \\ a^{\dagger}_{(-n)(-\boldsymbol{k})}(t), & \text{for } n < 0. \end{cases} \tag{39}$$

Thus, only half of all the $c_{n\boldsymbol{k}}(t)$ are independent dynamical variables.

The mode expansion of the electromagnetic fields in terms of $c_{n\boldsymbol{k}}(t)$ takes the compact form,

$$\boldsymbol{D}(\boldsymbol{r},t) = \sum_n \int_{\Omega_B} d\boldsymbol{k} c_{n\boldsymbol{k}}(t) \boldsymbol{D}_{n\boldsymbol{k}}(\boldsymbol{r}), \tag{40}$$

$$\boldsymbol{B}(\boldsymbol{r},t) = \sum_n \int_{\Omega_B} d\boldsymbol{k} c_{n\boldsymbol{k}}(t) \boldsymbol{B}_{n\boldsymbol{k}}(\boldsymbol{r}), \tag{41}$$

where the summations are performed over both positive and negative band indices n. We find such simple mode expansion formulas because the pairs of spatial field eigenmodes $(\boldsymbol{D}_{n\boldsymbol{k}}(\boldsymbol{r}), \boldsymbol{B}_{n\boldsymbol{k}}(\boldsymbol{r}))$ form a complete basis set in our dynamical space of all pairs of transverse fields $(\boldsymbol{D}(\boldsymbol{r},t), \boldsymbol{B}(\boldsymbol{r},t))$, taken at a given time t. The field expansion coefficients $c_{n\boldsymbol{k}}(t)$ can be expressed in terms of the fields and Bloch modes,

$$c_{n\boldsymbol{k}}(t) = \frac{1}{\hbar|\omega_{n\boldsymbol{k}}|} \int d\boldsymbol{r} \left\{ \frac{\boldsymbol{D}^*_{n\boldsymbol{k}}(\boldsymbol{r}) \cdot \boldsymbol{D}(\boldsymbol{r},t)}{\varepsilon_0 n^2(\boldsymbol{r})} + \frac{\boldsymbol{B}^*_{n\boldsymbol{k}}(\boldsymbol{r}) \cdot \boldsymbol{B}(\boldsymbol{r},t)}{\mu_0} \right\} \tag{42}$$

[cf. Eq. (35)]. Poisson brackets for the $c_{n\boldsymbol{k}}(t)$ immediately follow from Eqs. (39) and (38); we find

$$[c_{n\boldsymbol{k}}(t), c_{(-n')(-\boldsymbol{k}')}(t)] = \mathrm{sgn}(n)\, \delta_{nn'} \delta(\boldsymbol{k} - \boldsymbol{k}'). \tag{43}$$

Poisson brackets involving $c_{n\boldsymbol{k}}(t)$ and $c^{\dagger}_{n'\boldsymbol{k}'}(t)$ follow from this and from the fact that $c^{\dagger}_{n\boldsymbol{k}}(t) \equiv c_{(-n)(-\boldsymbol{k})}(t)$ (39), but we will not need to refer to the $c^{\dagger}_{n\boldsymbol{k}}(t)$ explicitly.

The part of the Hamiltonian describing linear dynamics [Eq. (10)] has a simple harmonic form in terms of either the $a_{n\boldsymbol{k}}(t)$ or the $c_{n\boldsymbol{k}}(t)$,

$$\begin{aligned} \mathcal{H}_0 &= \sum_{n>0} \int_{\Omega_B} d\boldsymbol{k} \hbar \omega_{n\boldsymbol{k}} a^{\dagger}_{n\boldsymbol{k}}(t) a_{n\boldsymbol{k}}(t) \\ &= \sum_n \int_{\Omega_B} d\boldsymbol{k} \frac{\hbar|\omega_{n\boldsymbol{k}}|}{2} c_{(-n)(-\boldsymbol{k})}(t) c_{n\boldsymbol{k}}(t), \end{aligned} \tag{44}$$

which follows from Eqs. (40), (41), and (35). The nonlinear part of the Hamiltonian $\mathcal{H}_{\mathrm{NL}}$, on the other hand, is much more conveniently expressed in terms of the $c_{n\boldsymbol{k}}(t)$. Thus we will use the $c_{n\boldsymbol{k}}(t)$ as the dynamical variables in the formulas to follow. The part of $\mathcal{H}_{\mathrm{NL}}$ that is third-order in $c_{n\boldsymbol{k}}(t)$ [the first term in Eq. (11)] is

$$\begin{aligned} \mathcal{H}^{(2)} = &- \frac{\hbar}{3\sqrt{8\pi^2}} \sum_{nn'n''} \int_{\Omega_B} d\boldsymbol{k}' \int_{\Omega_B} d\boldsymbol{k}'' \Gamma^{(2)}_{nn'n''}(\boldsymbol{k}', \boldsymbol{k}'') \\ &\times c_{n\lceil -\boldsymbol{k}' - \boldsymbol{k}'' \rfloor}(t) c_{n'\boldsymbol{k}'}(t) c_{n''\boldsymbol{k}''}(t), \end{aligned} \tag{45}$$

where $\lceil \boldsymbol{k} \rfloor$ denotes a "zone-wrapped" wave vector $\boldsymbol{k}$, that is, the wave vector in the first Brillouin zone Ω_B that corresponds to some arbitrary wave vector $\boldsymbol{k}$,

$$\lceil \boldsymbol{k} \rfloor \equiv \boldsymbol{k} - \boldsymbol{G}_{\boldsymbol{k}}, \text{ such that}$$

$$\lceil \boldsymbol{k} \rfloor \in \Omega_B, \ \forall \ \boldsymbol{k}, \tag{46}$$

with $\boldsymbol{G}_{\boldsymbol{k}}$ being one of the vectors of the reciprocal lattice, including $\boldsymbol{0}$. In deriving Eq. (45), we have used the discrete-Fourier-transform formula

$$\sum_{\boldsymbol{R}} \exp(-i\boldsymbol{\kappa} \cdot \boldsymbol{R}) = \frac{8\pi^3}{V_{\mathrm{cell}}} \sum_{\boldsymbol{G}} \delta(\boldsymbol{\kappa} + \boldsymbol{G}), \tag{47}$$

where V_{cell} is the volume of the unit cell of the photonic crystal, the summations are performed over all lattice vectors $\boldsymbol{R}$ and all reciprocal vectors $\boldsymbol{G}$ of the photonic crystal, and we have defined

$$\begin{aligned} &\Gamma^{(2)}_{nn'n''}(\boldsymbol{k}', \boldsymbol{k}'') \\ &\quad \equiv \frac{1}{\hbar\varepsilon_0} \int_{V_{\mathrm{cell}}} \frac{d\boldsymbol{r}}{V_{\mathrm{cell}}} \Gamma^{ijl}_2(\boldsymbol{r}) d^i_{n\lceil -\boldsymbol{k}' - \boldsymbol{k}'' \rfloor}(\boldsymbol{r}) d^j_{n'\boldsymbol{k}'}(\boldsymbol{r}) d^l_{n''\boldsymbol{k}''}(\boldsymbol{r}) \\ &\quad \times \exp[i(\boldsymbol{k}' + \boldsymbol{k}'' - \lceil \boldsymbol{k}' + \boldsymbol{k}'' \rfloor) \cdot \boldsymbol{r}]. \end{aligned} \tag{48}$$

Note that the combination of the wave vectors in the exponent is equal to $\boldsymbol{G}_{(\boldsymbol{k}'+\boldsymbol{k}'')}$, which is again one of the vectors of the reciprocal lattice. The quantities $\Gamma^{(2)}_{nn'n''}(\boldsymbol{k}', \boldsymbol{k}'')$ inherit symmetry properties from those of the $\boldsymbol{d}_{n\boldsymbol{k}}(\boldsymbol{r})$, which follow from the symmetry properties (28) and (33) of the $\boldsymbol{D}_{n\boldsymbol{k}}(\boldsymbol{r})$. We find

$$[\Gamma^{(2)}_{nn'n''}(\boldsymbol{k}', \boldsymbol{k}'')]^* = \Gamma^{(2)}_{nn'n''}(-\boldsymbol{k}', -\boldsymbol{k}''), \tag{49}$$

$$\begin{aligned} \Gamma^{(2)}_{nn'n''}(\boldsymbol{k}', \boldsymbol{k}'') &= \Gamma^{(2)}_{(-n)n'n''}(\boldsymbol{k}', \boldsymbol{k}'') = \Gamma^{(2)}_{n(-n')n''}(\boldsymbol{k}', \boldsymbol{k}'') \\ &= \Gamma^{(2)}_{nn'(-n'')}(\boldsymbol{k}', \boldsymbol{k}'') = \cdots. \end{aligned} \tag{50}$$

Here and below we use the shorthand "$=\cdots$" to indicate all other similar transformations of indices. As well, there is a band-index permutation symmetry of $\Gamma^{(2)}_{nn'n''}(\boldsymbol{k}', \boldsymbol{k}'')$ that follows from the Cartesian-index permutation symmetry of $\Gamma^{ijl}_2(\boldsymbol{r})$,

$$\Gamma^{(2)}_{nn'n''}(\boldsymbol{k}', \boldsymbol{k}'') = \Gamma^{(2)}_{nn''n'}(\boldsymbol{k}'', \boldsymbol{k}') = \Gamma^{(2)}_{n'nn''}(-\lceil \boldsymbol{k}' + \boldsymbol{k}'' \rfloor, \boldsymbol{k}'') = \cdots. \tag{51}$$

The expressions given here can be easily generalized to include higher order nonlinearities.

Hamilton's equations for the $c_{n\boldsymbol{k}}(t)$,

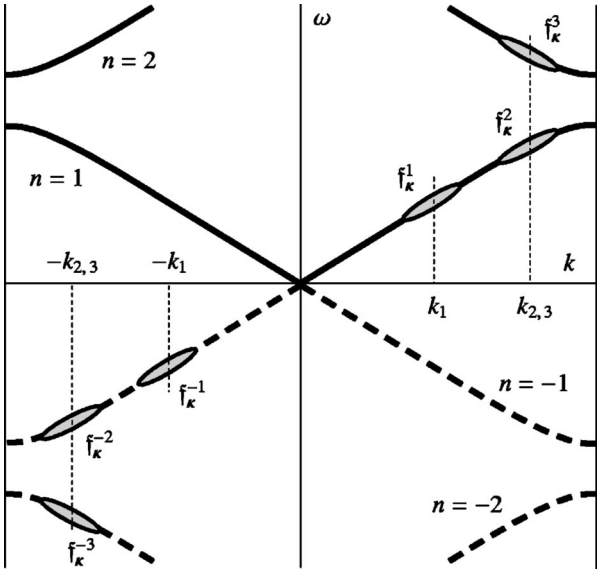

FIG. 2. Reciprocal-space envelope functions f^a_κ, where $\boldsymbol{\kappa}=[\boldsymbol{k}-\boldsymbol{k}_a]$, include the parts of the photonic bands marked by the shaded ovals. They represent the wave packets with $a=1$, 2, and 3 and their concomitant counterparts within the bands with negative n_a.

$$\frac{d}{dt}c_{n\boldsymbol{k}}(t)=\frac{1}{i\hbar}[c_{n\boldsymbol{k}}(t),\mathcal{H}], \tag{52}$$

lead to coupled equations for the $c_{n\boldsymbol{k}}(t)$; keeping terms up to those quadratic in $c_{n\boldsymbol{k}}(t)$, we find

$$\frac{d}{dt}c_{n\boldsymbol{k}}(t)=-i\omega_{n\boldsymbol{k}}c_{n\boldsymbol{k}}(t)+i\frac{\mathrm{sgn}(n)}{\sqrt{8\pi^3}}\sum_{n'n''}\int_{\Omega_B}d\boldsymbol{k}'\Gamma^{(2)}_{(-n)n''n'}(\lceil\boldsymbol{k}-\boldsymbol{k}'\rceil,\boldsymbol{k}')c_{n''\lceil\boldsymbol{k}-\boldsymbol{k}'\rceil}(t)c_{n'\boldsymbol{k}'}(t). \tag{53}$$

Recall that $\lceil\boldsymbol{k}\rceil$ is a zone-wrapped wave vector $\boldsymbol{k}$ (46). Higher-order nonlinearities can be included in the dynamical equation by a straightforward extension.

III. WAVE PACKETS AND EFFECTIVE FIELDS

A. Wave packets in reciprocal space

We now write our electromagnetic field as a superposition of wave packets numbered with index a. Each wave packet involves Bloch modes from a single band n_a, and all wave vectors associated with the wave packet are close to some central value $\boldsymbol{k}_a$. We refer to these as "formal" wave packets; a typical such wave packet labeled by a only contains spatial eigenmodes $\boldsymbol{D}_{n_a\boldsymbol{k}}(\boldsymbol{r})$ with $\boldsymbol{k}\in\Omega_a$, where Ω_a is the volume in the reciprocal space ("$\boldsymbol{k}$ space") that is centered around $\boldsymbol{k}_a$ and that represents the $\boldsymbol{k}$-space "footprint" of the wave packet. That is, the support of each of these formal wave packets is compact in $\boldsymbol{k}$ space. In Fig. 2 we shown 6 wave packets in 4 different photonic bands of a 1D photonic crystal by shaded ovals overlaying the parts of the bands that correspond to the modes $\boldsymbol{D}_{n_a\boldsymbol{k}}(\boldsymbol{r})$ comprising those wave packets.

Each $\boldsymbol{k}$-space volume Ω_a may wrap at the boundary of the first Brillouin zone Ω_B if $\boldsymbol{k}_a$ is sufficiently close to its boundary. This is illustrated by Ω_2 in the left plane of Fig. 3, that shows the first Brillouin zone of a 2D hexagonal lattice. The distance between $\boldsymbol{k}$ and $\boldsymbol{k}_a$ should be judged allowing for the wave vector wrapping at the zone boundary. We later exploit the small size of Ω_a relative to Ω_B by performing Taylor series expansions of fields at $\boldsymbol{k}_a$ and only retaining the most significant terms of the expansions, based on the multiple-scales analysis. To facilitate this approximate treatment, we introduce "local" wave vectors $\boldsymbol{\kappa}=[\boldsymbol{k}-\boldsymbol{k}_a]$, which are small compared to the maximum width of Ω_B. Each wave packet a associates a different $\boldsymbol{k}$ vector for a given $\boldsymbol{\kappa}$, since the central wave vector $\boldsymbol{k}_a$ enters into the definition of $\boldsymbol{\kappa}$. For $\boldsymbol{k}\in\Omega_a$ the corresponding local wave vectors $\boldsymbol{\kappa}\in\bar{\Omega}_a$, where $\bar{\Omega}_a$ is the wave-packet footprint volume in the $\boldsymbol{\kappa}$ space, centered around $\boldsymbol{\kappa}=0$. We assume that $\bar{\Omega}_a$ do not reach the boundaries the first Brillouin zone, since the diameters of $\bar{\Omega}_a$ are small.

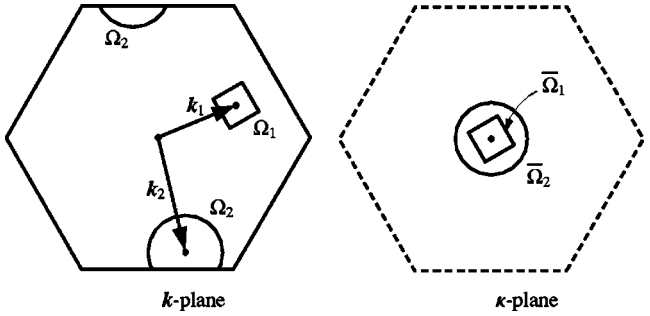

FIG. 3. Left: two wave-packet footprints Ω_a in the first Brillouin zone ($\boldsymbol{k}$ space); right: the wave-packet footprints $\bar{\Omega}_a$ in the space of local wave vectors $\boldsymbol{\kappa}=[\boldsymbol{k}-\boldsymbol{k}_a]$.

We choose the $\boldsymbol{k}$-space volumes Ω_a in such a way that different Ω_a and $\Omega_{a'}$ do not overlap if the wave packets belong to the same photonic band $n_a=n_{a'}$. This condition can be formally expressed as

$$\delta_{n_an_{a'}}\Pi_a(\lceil\boldsymbol{k}-\boldsymbol{k}_a\rceil)\Pi_{a'}(\lceil\boldsymbol{k}-\boldsymbol{k}_{a'}\rceil)=\delta_{aa'}\Pi_a(\lceil\boldsymbol{k}-\boldsymbol{k}_a\rceil), \tag{54}$$

where $\Pi_a(\boldsymbol{\kappa})$ is a "filter" function, defined as

$$\Pi_a(\boldsymbol{\kappa})=\begin{cases}1, & \text{for } \boldsymbol{\kappa}\in\bar{\Omega}_a,\\ 0, & \text{for } \boldsymbol{\kappa}\notin\bar{\Omega}_a,\end{cases} \tag{55}$$

and the condition $\boldsymbol{\kappa}\in\bar{\Omega}_a$ is equivalent to $\boldsymbol{k}\in\Omega_a$.

In principle one could organize an arbitrary initial state of the electromagnetic field with the aid of these formal wave packets, by first completely covering the Brillouin zone with a set of nonoverlapping volumes Ω_a for each band, identifying a formal wave packet centered at each $\boldsymbol{k}_a$, and then sorting the different Bloch components of the electromagnetic field into these wave packets. In practice, of course, one is often interested in a one or a few *physical* wave packets, often taken to be Gaussian in form for simplicity, that are centered at different wave vectors. Strictly speaking, a Gaussian wave packet will extend to wave vectors outside any finite volume in reciprocal space, such as the volumes Ω_a. Nonetheless, in many cases of interest it is possible to define Ω_a large enough so that, while still a small fraction of

the volume of the Brillouin zone, essentially the full Gaussian wave packet is contained within in. But if this is not the case, the electromagnetic field in a single physical wave packet can be divided into as many formal wave packets as necessary to achieve a good approximation. The theory we develop below allows for the interaction of these formal wave packets. Propagation of a single physical wave packet can, if necessary, be treated as the propagation and interaction of a set of formal wave packets. Even if this is not thought necessary, and it is supposed that a given physical wave packet can be well-approximated by a single formal wave packet, such a more general treatment could be implemented to check the quality of the approximation.

We number the wave packets so that

$$\mathrm{sgn}(a) = \mathrm{sgn}(n_a), \tag{56}$$

and we include the wave packet $(-a)$, whose constituent modes are complex conjugates of the modes forming the wave packet a, to guarantee that the electric field is real. These concomitant wave packets, one at $(-a)$ for each wave packet at a, are described by the parameters

$$n_{(-a)} = -n_a, \tag{57}$$

$$\boldsymbol{k}_{(-a)} = -\boldsymbol{k}_a, \tag{58}$$

$$\Pi_{(-a)}(-\boldsymbol{\kappa}) = \Pi_a(\boldsymbol{\kappa}). \tag{59}$$

We now introduce positive-index reciprocal-space envelope functions $\mathfrak{g}^a_{\boldsymbol{\kappa}}(t)$ that represent the contribution of the wave packet $a>0$ to the field expansion coefficient $a_{n_a\boldsymbol{k}}(t)$,

$$\mathfrak{g}^a_{\boldsymbol{\kappa}}(t) = \Pi_a(\boldsymbol{\kappa}) a_{n_a\lceil \boldsymbol{k}_a+\boldsymbol{\kappa}\rceil}(t). \tag{60}$$

Using this definition, we can write the $a_{n\boldsymbol{k}}(t)$ as

$$a_{n\boldsymbol{k}}(t) = \sum_a \delta_{nn_a} \mathfrak{g}^a_{\lceil \boldsymbol{k}-\boldsymbol{k}_a\rceil}(t). \tag{61}$$

The zone-wrapped wave vector $\lceil \boldsymbol{k}-\boldsymbol{k}_a\rceil$ in (61) reflects the fact that, for $\boldsymbol{k}_a$ close to the boundary of the first Brillouin zone, some wave vectors $\boldsymbol{k}$ of the wave packet can be located on the opposite side of the Brillouin zone.

The Poisson bracket for $\mathfrak{g}^a_{\boldsymbol{\kappa}}(t)$,

$$[\mathfrak{g}^a_{\boldsymbol{\kappa}}(t), (\mathfrak{g}^{a'}_{\boldsymbol{\kappa}'}(t))^\dagger] = \delta_{aa'}\Pi_a(\boldsymbol{\kappa})\delta(\boldsymbol{\kappa}-\boldsymbol{\kappa}'), \tag{62}$$

follows from Eq. (38), taking into account the definition of $\mathfrak{g}^a_{\boldsymbol{\kappa}}(t)$ (60) and the nonoverlapping of the same-band wave packets [see Eq. (54)]. This is similar to what has been done earlier [6], but there only one wave packet per photonic band was considered, and thus the introduction of the filter function (55) was not necessary. As a result, there was no filter function $\Pi_a(\boldsymbol{\kappa})$ appearing in the commutation relation corresponding to Eq. (62). Our Eq. (62) is a generalization of that work [6] necessary to treat a number of wave packets in the same band.

As with the field expansion coefficients, it is convenient to introduce reciprocal-space envelope functions $\mathfrak{f}^a_{\boldsymbol{\kappa}}(t)$ that can accept both positive and negative wave-packet indices a,

$$\mathfrak{f}^a_{\boldsymbol{\kappa}}(t) \equiv \begin{cases} \mathfrak{g}^a_{\boldsymbol{\kappa}}(t), & \text{for } a>0, \\ (\mathfrak{g}^{(-a)}_{(-\boldsymbol{\kappa})}(t))^\dagger, & \text{for } a<0, \end{cases} \tag{63}$$

and using Eq. (39) we see that

$$\mathfrak{f}^a_{\boldsymbol{\kappa}}(t) = \Pi_a(\boldsymbol{\kappa}) c_{n_a\lceil \boldsymbol{k}_a+\boldsymbol{\kappa}\rceil}(t) \tag{64}$$

for both positive and negative a; this is illustrated in Fig. 2. The Poisson bracket for $\mathfrak{f}^a_{\boldsymbol{\kappa}}(t)$ immediately follows:

$$[\mathfrak{f}^a_{\boldsymbol{\kappa}}(t), \mathfrak{f}^{(-a')}_{(-\boldsymbol{\kappa}')}(t)] = \mathrm{sgn}(a)\,\delta_{aa'}\Pi_a(\boldsymbol{\kappa})\delta(\boldsymbol{\kappa}-\boldsymbol{\kappa}'). \tag{65}$$

The introduction of the reciprocal-space envelope functions allows us to separate the field itself into distinct wave-packet contributions. Using Eq. (40) and the definition of $\mathfrak{f}^a_{\boldsymbol{\kappa}}(t)$, the field $\boldsymbol{D}(\boldsymbol{r},t)$ can now be written as a superposition of the field wave packets $\boldsymbol{D}_a(\boldsymbol{r},t)$,

$$\boldsymbol{D}(\boldsymbol{r},t) = \sum_a \boldsymbol{D}_a(\boldsymbol{r},t), \tag{66}$$

where

$$\boldsymbol{D}_a(\boldsymbol{r},t) = \int_{\Omega_B} d\boldsymbol{k}\, \mathfrak{f}^a_{\lceil \boldsymbol{k}-\boldsymbol{k}_a\rceil}(t)\boldsymbol{D}_{n_a\boldsymbol{k}}(\boldsymbol{r}). \tag{67}$$

The field wave packets $\boldsymbol{D}_a(\boldsymbol{r},t)$ have the obvious symmetry,

$$\boldsymbol{D}_{(-a)}(\boldsymbol{r},t) = [\boldsymbol{D}_a(\boldsymbol{r},t)]^\dagger, \tag{68}$$

which ensures the reality of the electric field.

B. Formal wave packet dynamics

We can now turn to the dynamical evolution of these wave packets. The part of the Hamiltonian describing linear dynamics [Eq. (44)] is expressed in terms of the reciprocal-space envelope functions $\mathfrak{f}^a_{\boldsymbol{\kappa}}(t)$ using Eq. (64),

$$\mathcal{H}_0 = \sum_a \int_{\Omega_B} d\boldsymbol{\kappa} \frac{\hbar|\overline{\omega^a_{\boldsymbol{\kappa}}}|}{2} \mathfrak{f}^{(-a)}_{(-\boldsymbol{\kappa})}(t)\mathfrak{f}^a_{\boldsymbol{\kappa}}(t), \tag{69}$$

where the summation extends to both positive and negative a, and we have defined

$$\overline{\omega^a_{\boldsymbol{\kappa}}} \equiv \omega_{n_a\lceil \boldsymbol{k}_a+\boldsymbol{\kappa}\rceil}. \tag{70}$$

Writing the part of the Hamiltonian describing the quadratic optical response [Eq. (45)] also in terms of the reciprocal-space envelope functions $\mathfrak{f}^a_{\boldsymbol{\kappa}}(t)$, we find

$$\mathcal{H}^{(2)} = -\frac{\hbar}{3\sqrt{8\pi^3}} \sum_{aa'a''} \int_{\Omega_B} d\boldsymbol{\kappa}' \int_{\Omega_B} d\boldsymbol{\kappa}'' \gamma^{(2)}_{aa'a''}(\boldsymbol{\kappa}', \boldsymbol{\kappa}'') \times \mathfrak{f}^a_{(-\lceil \boldsymbol{\kappa}'+\boldsymbol{\kappa}''+\boldsymbol{\Delta}^{(2)}_{aa'a''}\rceil)}(t)\mathfrak{f}^{a'}_{\boldsymbol{\kappa}'}(t)\mathfrak{f}^{a''}_{\boldsymbol{\kappa}''}(t), \tag{71}$$

where the mismatch of the central wave vectors of the wave packets a, a', and a'' is denoted as

$$\boldsymbol{\Delta}^{(2)}_{aa'a''} \equiv \boldsymbol{k}_a + \boldsymbol{k}_{a'} + \boldsymbol{k}_{a''}, \tag{72}$$

and

$$\gamma^{(2)}_{aa'a''}(\boldsymbol{\kappa}',\boldsymbol{\kappa}'') \equiv \Gamma^{(2)}_{n_a n_{a'} n_{a''}}([\boldsymbol{k}_{a'}+\boldsymbol{\kappa}'],[\boldsymbol{k}_{a''}+\boldsymbol{\kappa}'']). \quad (73)$$

The $\gamma^{(2)}_{aa'a''}(\boldsymbol{\kappa}',\boldsymbol{\kappa}'')$ inherit a set of symmetry properties from the $\Gamma^{(2)}_{nn'n''}(\boldsymbol{k}',\boldsymbol{k}'')$; from Eqs. (49) and (50) we find

$$[\gamma^{(2)}_{aa'a''}(\boldsymbol{\kappa}',\boldsymbol{\kappa}'')]^* = \gamma^{(2)}_{(-a)(-a')(-a'')}(-\boldsymbol{\kappa}',-\boldsymbol{\kappa}''), \quad (74)$$

$$\gamma^{(2)}_{aa'a''}(\boldsymbol{\kappa}',\boldsymbol{\kappa}'') = \gamma^{(2)}_{(-a)a'a''}(\boldsymbol{\kappa}',\boldsymbol{\kappa}'') = \gamma^{(2)}_{a(-a')a''}([\boldsymbol{\kappa}'+2\boldsymbol{k}_{a'}],\boldsymbol{\kappa}'') = \gamma^{(2)}_{aa'(-a'')}(\boldsymbol{\kappa}',[\boldsymbol{\kappa}''+2\boldsymbol{k}_{a''}]) = \cdots, \quad (75)$$

while the permutation symmetry of $\gamma^{(2)}_{aa'a''}(\boldsymbol{\kappa}',\boldsymbol{\kappa}'')$ follows directly from Eq. (51),

$$\gamma^{(2)}_{aa'a''}(\boldsymbol{\kappa}',\boldsymbol{\kappa}'') = \gamma^{(2)}_{aa''a'}(\boldsymbol{\kappa}'',\boldsymbol{\kappa}') = \gamma^{(2)}_{a'aa''}(-[\boldsymbol{\kappa}'+\boldsymbol{\kappa}''+\boldsymbol{\Delta}^{(2)}_{aa'a''}],\boldsymbol{\kappa}'') = \cdots. \quad (76)$$

In treating this second-order interaction, we assume that to good approximation the material polarization created by a pair of wave packets a' and a'' will only affect a limited number of wave packets a, the set of which we denote as $\mathfrak{A}^{(2)}(a',a'')$. Consequently, the wave packets a' and a'' should appear in some terms in the nonlinear Hamiltonian together with the wave packet $(-a)$. In most cases, every set $\mathfrak{A}^{(2)}(a',a'')$ contains two wave packets a that belong to two photonic bands differing by the polarization of their modes. Obviously, the set $\mathfrak{A}^{(2)}(a',a'')$ is not empty if the second-order nonlinear interaction between the wave packets a' and a'' actually occurs.

From a formal point of view, it would be hard to achieve the self-consistency of our set of interacting wave packets without extending them to all $\boldsymbol{k}$-vectors in all photonic bands. Even with the assumption that each actual wave packet in the photonic crystal is well described by the $\boldsymbol{k}$ vectors within a given formal wave packet, we would have to take into account the effects of the nonlinear interaction where the wave packets a, a', and a'' are combined in all different ways. That is, not only $[\boldsymbol{k}'+\boldsymbol{k}'']$ should be in some Ω_a, $a \in \mathfrak{A}^{(2)}(a',a'')$ for every pair of Bloch modes with $\boldsymbol{k}' \in \Omega_{a'}$ and $\boldsymbol{k}'' \in \Omega_{a''}$ that participate in the second-order interaction, but our set of wave packets should also contain all the Bloch modes that may appear in the interaction of any wave packet containing Bloch modes with wave vectors $[\boldsymbol{k}'+\boldsymbol{k}''] \in \Omega_a$, and so on. In practice, of course, the wave packets that become important are restricted by phase-matching considerations. In this respect the interaction of wave packets in photonic crystals resembles that of wave packets in uniform media, except of course that in photonic crystals those phase-matching conditions can have much richer consequences. We will see below how phase-matching limits the number of wave packets we need consider; for the moment we assume that those considerations restrict us in practice to a finite set. Note that since concomitant wave packets a and $(-a)$ are always present in pairs, and because of the symmetries discussed above, from $a \in \mathfrak{A}^{(2)}(a',a'')$ follows $(-a) \in \mathfrak{A}^{(2)}(-a',-a'')$. With our choice of wave packets, the sum over all a in Eq. (71) can be replaced with a sum over $a \in \mathfrak{A}^{(2)}(-a',-a'')$.

The equation of motion for $\mathfrak{f}^a_{\boldsymbol{\kappa}}(t)$, written here up to the terms quadratic in $\mathfrak{f}^a_{\boldsymbol{\kappa}}(t)$, follows directly from Eq. (53) and the definition of $\mathfrak{f}^a_{\boldsymbol{\kappa}}(t)$ (64):

$$\frac{d}{dt}\mathfrak{f}^a_{\boldsymbol{\kappa}}(t) = -i\bar{\omega}^a_{\boldsymbol{\kappa}}\mathfrak{f}^a_{\boldsymbol{\kappa}}(t) + i\frac{\mathrm{sgn}(a)}{\sqrt{8\pi^3}} \sum_{\substack{a'a'': \\ a\in\mathfrak{A}^{(2)}(a',a'')}} \int_{\Omega_B} d\boldsymbol{\kappa}'\, \gamma^{(2)}_{(-a)a''a'}(\boldsymbol{\kappa} - \boldsymbol{\kappa}' - \boldsymbol{\Delta}^{(2)}_{(-a)a''a'},\boldsymbol{\kappa}')\mathfrak{f}^{a''}_{(\boldsymbol{\kappa}-\boldsymbol{\kappa}'-\boldsymbol{\Delta}^{(2)}_{(-a)a''a'})}(t)\mathfrak{f}^{a'}_{\boldsymbol{\kappa}'}(t). \quad (77)$$

In this equation we have omitted the zone-wrapping notation $[\ldots]$, assuming that the wave packets (and hence $\boldsymbol{\kappa}$'s) are reasonably small in the $\boldsymbol{k}$-space and that the wave-vector mismatch $\boldsymbol{\Delta}^{(2)}_{(-a)a''a'}$ is also small.

C. Effective fields and their properties

We now move from reciprocal space to real space and introduce effective fields associated with the formal wave packets introduced in Sec. III A. We define the effective field of a wave packet a as a Fourier transform of its reciprocal-space envelope function $\mathfrak{g}^a_{\boldsymbol{\kappa}}(t)$ or $\mathfrak{f}^a_{\boldsymbol{\kappa}}(t)$. To do this we can restrict ourselves to positive a and an analysis based on $\mathfrak{g}^a_{\boldsymbol{\kappa}}(t)$, using complex or Hermitian conjugates for negative-index wave packets. For $a>0$, then, we introduce positive-index effective fields,

$$g_a(\boldsymbol{r},t) = \int_{\Omega_B} \frac{d\boldsymbol{\kappa}}{\sqrt{8\pi^3}} \mathfrak{g}^a_{\boldsymbol{\kappa}}(t)\exp(i\boldsymbol{\kappa}\cdot\boldsymbol{r}). \quad (78)$$

The Poisson brackets involving the $g_a(\boldsymbol{r},t)$ are obtained from the Poisson brackets involving the $\mathfrak{g}^a_{\boldsymbol{\kappa}}(t)$ (62),

$$[g_a(\boldsymbol{r},t),g^\dagger_{a'}(\boldsymbol{r}',t)] = \delta_{aa'}\tilde{\Pi}_a(\boldsymbol{r}-\boldsymbol{r}'), \quad (79)$$

where

$$\tilde{\Pi}_a(\boldsymbol{r}) \equiv \frac{1}{8\pi^3}\int_{\Omega_B} d\boldsymbol{\kappa}\Pi_a(\boldsymbol{\kappa})\exp(i\boldsymbol{\kappa}\cdot\boldsymbol{r}) \quad (80)$$

is a "space filter function" that filters a given wave packet out of all same-band wave packets. The appearance of a filter function $\tilde{\Pi}_a(\boldsymbol{r}-\boldsymbol{r}')$ rather than a Dirac delta function in Eq. (79) is a consequence of our division of reciprocal space into a set of wave packet regions.

We also introduce the effective fields $f_a(\boldsymbol{r},t)$ that can accept both positive and negative wave-packet indices a,

$$f_a(\boldsymbol{r},t) \equiv \begin{cases} g_a(\boldsymbol{r},t), & \text{for } a>0, \\ g^\dagger_{(-a)}(\boldsymbol{r},t), & \text{for } a<0, \end{cases} \quad (81)$$

from which it follows that

$$f_a(\boldsymbol{r},t) = \int_{\Omega_B} \frac{d\boldsymbol{\kappa}}{\sqrt{8\pi^3}} \mathfrak{f}^a_{\boldsymbol{\kappa}}(t)\exp(i\boldsymbol{\kappa}\cdot\boldsymbol{r}) \quad (82)$$

for both positive and negative a. The Poisson bracket for $f_a(\boldsymbol{r},t)$ follows from Eq. (79),

$$[f_a(\boldsymbol{r},t), f_{(-a')}(\boldsymbol{r}',t)] = \mathrm{sgn}(a)\,\delta_{aa'}\widetilde{\Pi}_a(\boldsymbol{r}-\boldsymbol{r}'). \tag{83}$$

Using the inverse Fourier transform of $f_a(\boldsymbol{r},t)$, we express the field wave packet (67) in terms of the effective field:

$$\boldsymbol{D}_a(\boldsymbol{r},t) = \int \frac{d\boldsymbol{r}'}{\sqrt{8\pi^3}} f_a(\boldsymbol{r}',t) \int_{\Omega_\mathrm{B}} d\boldsymbol{\kappa} \boldsymbol{D}_{n_a[\boldsymbol{k}_a+\boldsymbol{\kappa}]}(\boldsymbol{r}) \exp(-i\boldsymbol{\kappa}\cdot\boldsymbol{r}'). \tag{84}$$

Note that instead of Ω_B we could use any volume in the $\boldsymbol{\kappa}$-space that contains $\overline{\Omega}_a$, so there remains some freedom in specifying the "kernel" of the transformation from the effective field to the actual electric field.

One of the reasons for introducing the effective fields $f_a(\boldsymbol{r},t)$ is to benefit from series expansions at $\boldsymbol{\kappa}=\boldsymbol{0}$ that we will now undertake. The idea is that a well-localized $\boldsymbol{D}_a(\boldsymbol{r},t)$ consisting of contributions from a narrow range of $\boldsymbol{\kappa}$ (67) can be described by a smoothly varying $f_a(\boldsymbol{r},t)$. This only follows, of course, if the Bloch functions $\boldsymbol{D}_{n_a\boldsymbol{k}}(\boldsymbol{r})$ are slowly varying over Ω_a; if Ω_a is split at the boundary of the first Brillouin zone, this is understood as the $\boldsymbol{D}_{n_a[\boldsymbol{k}_a+\boldsymbol{\kappa}]}(\boldsymbol{r})$ being slowly varying in the $\overline{\Omega}_a$. If Ω_a is small and there are no points, lines, or surfaces of degeneracy that involve the band n_a in Ω_a, this can be achieved by suitably choosing the phase of $\boldsymbol{D}_{n_a\boldsymbol{k}}(\boldsymbol{r})$ at every $\boldsymbol{k}$ through, for example, a $k\cdot p$ type of expansion about $\boldsymbol{k}_a$ [14,15]. With degeneracies in Ω_a that involve the band n_a the problem is more complicated; we will not address it here, but plan to turn to it in a future communication.

To see how such a series expansion can be introduced into a description of the dynamics, we begin with the part of the Hamiltonian describing the linear response. We use the expansion

$$\overline{\omega}^a_{\boldsymbol{\kappa}} = \omega_a + \omega_a^{(i)}\kappa^i + \frac{1}{2}\omega_a^{(ij)}\kappa^i\kappa^j + \cdots, \tag{85}$$

where

$$\omega_a \equiv \omega_{n_a\boldsymbol{k}_a} = -\omega_{(-a)}, \tag{86}$$

$$\omega_a^{(i)} \equiv \left.\frac{\partial\omega_{n_a\boldsymbol{k}}}{\partial k^i}\right|_{\boldsymbol{k}=\boldsymbol{k}_a} = \omega^{(i)}_{(-a)}, \tag{87}$$

$$\omega_a^{(ij)} \equiv \left.\frac{\partial^2\omega_{n_a\boldsymbol{k}}}{\partial k^i\partial k^j}\right|_{\boldsymbol{k}=\boldsymbol{k}_a} = -\omega^{(ij)}_{(-a)}, \quad \text{etc.} \tag{88}$$

The second series coefficient is the group-velocity vector of the wave packet a: $v_a^i \equiv \omega_a^{(i)}$. The third coefficient $\omega_a^{(ij)}$ is obviously symmetric with respect to the permutation of its indices i and j. Then we can write $\mathcal{H}_0$ in the form of a volume integral of the sum of the contributions $\widetilde{h}_{0a}(\boldsymbol{r},t)$ from separate wave packets a,

$$\mathcal{H}_0 = \sum_a \int d\boldsymbol{r}\widetilde{h}_{0a}(\boldsymbol{r},t), \tag{89}$$

where in the expression for $\widetilde{h}_{0a}(\boldsymbol{r},t)$ we rely on the series expansion of $\overline{\omega}^a_{\boldsymbol{\kappa}}$ up to the second order in $\boldsymbol{\kappa}$,

$$\widetilde{h}_{0a}(\boldsymbol{r},t) = \frac{\hbar|\omega_a|}{2}\Bigg[f_{(-a)}(\boldsymbol{r},t)f_a(\boldsymbol{r},t) + i\frac{\omega_a^{(i)}}{2\omega_a}\left(\frac{\partial f_{(-a)}(\boldsymbol{r},t)}{\partial r^i} f_a(\boldsymbol{r},t) - f_{(-a)}(\boldsymbol{r},t)\frac{\partial f_a(\boldsymbol{r},t)}{\partial r^i}\right) + \frac{\omega_a^{(ij)}}{2\omega_a}\frac{\partial f_{(-a)}(\boldsymbol{r},t)}{\partial r^i}\frac{\partial f_a(\boldsymbol{r},t)}{\partial r^j} + \cdots\Bigg]. \tag{90}$$

As we will show later, this $\widetilde{h}_{0a}(\boldsymbol{r},t)$ can be considered a linear part of the averaged energy density of the electromagnetic field, attributed to the wave packet a. We define it here to be Hermitian,

$$[\widetilde{h}_{0a}(\boldsymbol{r},t)]^\dagger = \widetilde{h}_{0a}(\boldsymbol{r},t), \tag{91}$$

although it is not necessary, since $\widetilde{h}_{0a}(\boldsymbol{r},t)$ and $\widetilde{h}_{0(-a)}(\boldsymbol{r},t) = [\widetilde{h}_{0a}(r,t)]^\dagger$ always appear together in Eq. (89). The approximation involved in truncating Eq. (85) when deriving Eq. (90) can be characterized formally, in the multiple-scales sense, by introducing small parameters that identify the ratio of $\omega_a^{(i)}/2\omega_a$ to the distance over which the functions $f_a(\boldsymbol{r},t)$ vary, and of the ratio of $\omega_a^{(ij)}/2\omega_a$ to the square of that distance, *etc*. We will not perform that formal multiple-scales analysis here.

An approximate expression for $\mathcal{H}^{(2)}$, following from Eq. (71), can also be written as a volume integral,

$$\mathcal{H}^{(2)} = \int d\boldsymbol{r}\widetilde{h}^{(2)}(\boldsymbol{r},t), \tag{92}$$

where

$$\widetilde{h}^{(2)}(\boldsymbol{r},t) = -\frac{\hbar}{3} \sum_{\substack{aa'a'':\\ (-a)\in\mathfrak{A}^{(2)}(a',a'')}} \overline{\gamma}^{(2)}_{aa'a''} f_a(\boldsymbol{r},t)f_{a'}(\boldsymbol{r},t)f_{a''}(\boldsymbol{r},t) \times \exp(i\boldsymbol{\Delta}^{(2)}_{aa'a''}\cdot\boldsymbol{r}), \tag{93}$$

and for $\gamma^{(2)}_{aa'a''}(\boldsymbol{\kappa}',\boldsymbol{\kappa}'')$ we have adopted the approximation

$$\gamma^{(2)}_{aa'a''}(\boldsymbol{\kappa}',\boldsymbol{\kappa}'') \approx \gamma^{(2)}_{aa'a''}\left(-\frac{1}{3}\boldsymbol{\Delta}^{(2)}_{aa'a''}, -\frac{1}{3}\boldsymbol{\Delta}^{(2)}_{aa'a''}\right) \equiv \overline{\gamma}^{(2)}_{aa'a''}. \tag{94}$$

The reason for using $-\frac{1}{3}\boldsymbol{\Delta}^{(2)}_{aa'a''}$ in this definition is to make $\overline{\gamma}^{(2)}_{aa'a''}$ more symmetric, so that

$$[\overline{\gamma}^{(2)}_{aa'a''}]^* = \overline{\gamma}^{(2)}_{(-a)(-a')(-a'')}, \tag{95}$$

$$\bar{\gamma}^{(2)}_{aa'a''} = \bar{\gamma}^{(2)}_{aa''a'} = \bar{\gamma}^{(2)}_{a'aa''} = \cdots, \tag{96}$$

thus simplifying our subsequent formulas. Corrections over Eq. (94) to $\gamma^{(2)}_{aa'a''}(\boldsymbol{\kappa}', \boldsymbol{\kappa}'')$ can be introduced, again in a multiple-scales analysis, but we will here keep only the lowest order contribution $\bar{\gamma}^{(2)}_{aa'a''}$ to $\gamma^{(2)}_{aa'a''}(\boldsymbol{\kappa}', \boldsymbol{\kappa}'')$, under the assumption that the nonlinearity is weak and its effect is at most of the order of the group-velocity-dispersion term in Eq. (90). The term $\tilde{h}^{(2)}(\boldsymbol{r}, t)$ is Hermitian because of the symmetry properties of $\bar{\gamma}^{(2)}_{aa'a''}$ (95) and (96). Note that $\tilde{h}^{(2)}(\boldsymbol{r}, t)$ cannot be separated into contributions from different wave packets, but rather represents the contribution of the wave-packet interaction to the averaged energy density.

The equation of motion for the $f_a(\boldsymbol{r}, t)$ is now obtained either by taking a Fourier transform of the equation of motion for $\mathfrak{f}^a_{\boldsymbol{\kappa}}(t)$ (77) or from the Hamilton equation,

$$\frac{\partial}{\partial t} f_a(\boldsymbol{r}, t) = \frac{1}{i\hbar}[f_a(\boldsymbol{r}, t), \mathcal{H}], \tag{97}$$

and it is as follows:

$$\begin{aligned}\frac{\partial}{\partial t} f_a(\boldsymbol{r}, t) = &- i\omega_a f_a(\boldsymbol{r}, t) - \omega^{(i)}_a \frac{\partial f_a(\boldsymbol{r}, t)}{\partial r^i} + \frac{i}{2}\omega^{(ij)}_a \frac{\partial^2 f_a(\boldsymbol{r}, t)}{\partial r^i \partial r^j} + \cdots \\ &+ i\,\mathrm{sgn}(a) \sum_{\substack{a'a'': \\ a \in \mathfrak{A}^{(2)}(a', a'')}} \bar{\gamma}^{(2)}_{(-a)a'a''} f_{a'}(\boldsymbol{r}, t) f_{a''}(\boldsymbol{r}, t) \\ &\times \exp(i\boldsymbol{\Delta}^{(2)}_{(-a)a'a''} \cdot \boldsymbol{r}).\end{aligned} \tag{98}$$

In deriving this equation of motion, we have used the expression (83) for the Poisson bracket for $f_a(\boldsymbol{r}, t)$, which does not include a Dirac δ-function. From the Poisson bracket the Fourier transform of the nonlinear part of the equation acquires a factor of $\Pi_a(\boldsymbol{\kappa})$; this is equivalent to the condition $a \in \mathfrak{A}^{(2)}(a', a'')$ we impose on the summation over the wave packets. This condition naturally "directs" the nonlinearly generated field to appropriate wave packets; if we would have a Dirac δ-function Poisson bracket, we would have to assign the nonlinear contributions to different wave packets "by hand," from physical and convenience considerations.

In many cases it is convenient to introduce a slowly-varying effective field $\bar{f}_a(\boldsymbol{r}, t)$,

$$f_a(\boldsymbol{r}, t) = \bar{f}_a(\boldsymbol{r}, t) \exp(-i\bar{\omega}_a t), \tag{99}$$

where $\bar{\omega}_a$ is a "carrier frequency" that can be chosen later for convenience. The equation of motion for $\bar{f}_a(\boldsymbol{r}, t)$ then takes the form

$$\begin{aligned}\left(\frac{\partial}{\partial t} + v^i_a \frac{\partial}{\partial r^i}\right)\bar{f}_a(\boldsymbol{r}, t) = &- i(\omega_a - \bar{\omega}_a)\bar{f}_a(\boldsymbol{r}, t) + \frac{i}{2}\omega^{(ij)}_a \frac{\partial^2 \bar{f}_a(\boldsymbol{r}, t)}{\partial r^i \partial r^j} \\ &+ \cdots + i\,\mathrm{sgn}(a) \sum_{\substack{a'a'': \\ a \in \mathfrak{A}^{(2)}(a', a'')}} \bar{\gamma}^{(2)}_{(-a)a'a''} \\ &\times \bar{f}_{a'}(\boldsymbol{r}, t) \bar{f}_{a''}(\boldsymbol{r}, t) \exp[i(\bar{\omega}_a - \bar{\omega}_{a'} - \bar{\omega}_{a''})t \\ &+ i\boldsymbol{\Delta}^{(2)}_{(-a)a'a''} \cdot \boldsymbol{r}].\end{aligned} \tag{100}$$

By suitably choosing $\bar{\omega}_a$ and $\boldsymbol{k}_a$, we can eliminate some of the terms $(\omega_a - \bar{\omega}_a)$, $(\bar{\omega}_a - \bar{\omega}_{a'} - \bar{\omega}_{a''})$, and $\boldsymbol{\Delta}^{(2)}_{(-a)a'a''}$, but cannot generally eliminate all of them.

D. Continuity equation

To approximately describe the energy distribution of the electromagnetic field, we introduce the effective energy density consisting of the linear and nonlinear contributions defined in Eqs. (90) and (93),

$$\tilde{h}(\boldsymbol{r}, t) = \sum_a \tilde{h}_{0a}(\boldsymbol{r}, t) + \tilde{h}^{(2)}(\boldsymbol{r}, t), \tag{101}$$

where the nonlinearity here is only accounted for up to the second order. The effective energy density $\tilde{h}(\boldsymbol{r}, t)$ satisfies the continuity equation,

$$\frac{\partial \tilde{h}(\boldsymbol{r}, t)}{\partial t} = -\,\boldsymbol{\nabla} \cdot \tilde{\boldsymbol{s}}(\boldsymbol{r}, t), \tag{102}$$

exactly, where the effective Poynting vector $\tilde{\boldsymbol{s}}(\boldsymbol{r}, t)$, like $\tilde{h}(\boldsymbol{r}, t)$, is a sum of linear contributions from separate wave packets and nonlinear "interaction" terms,

$$\tilde{\boldsymbol{s}}(\boldsymbol{r}, t) = \sum_a \tilde{\boldsymbol{s}}_{0a}(\boldsymbol{r}, t) + \tilde{\boldsymbol{s}}^{(2)}(\boldsymbol{r}, t). \tag{103}$$

Here the linear effective Poynting vector of the wave packet a is

$$\begin{aligned}\tilde{s}^i_{0a}(\boldsymbol{r}, t) = \frac{\hbar|\omega_a|}{2}\Bigg[&\omega^{(i)}_a f_{(-a)}(\boldsymbol{r}, t) f_a(\boldsymbol{r}, t) + i\frac{\omega^{(i)}_a \omega^{(j)}_a + \omega_a \omega^{(ij)}_a}{2\omega_a}\left(\frac{\partial f_{(-a)}(\boldsymbol{r}, t)}{\partial r^j} f_a(\boldsymbol{r}, t) - f_{(-a)}(\boldsymbol{r}, t)\frac{\partial f_a(\boldsymbol{r}, t)}{\partial r^j}\right) \\ &+ \frac{\omega^{(i)}_a \omega^{(jk)}_a}{\omega_a}\left(\frac{\partial f_{(-a)}(\boldsymbol{r}, t)}{\partial r^j}\frac{\partial f_a(\boldsymbol{r}, t)}{\partial r^k}\right) + \frac{\omega^{(i)}_a \omega^{(jk)}_a - 2\omega^{(ij)}_a \omega^{(k)}_a}{4\omega_a}\left(\frac{\partial^2 f_{(-a)}(\boldsymbol{r}, t)}{\partial r^j \partial r^k} f_a(\boldsymbol{r}, t) + f_{(-a)}(\boldsymbol{r}, t)\frac{\partial^2 f_a(\boldsymbol{r}, t)}{\partial r^j \partial r^k}\right) \\ &+ i\frac{\omega^{(ij)}_a \omega^{(kl)}_a}{4\omega_a}\left(\frac{\partial^2 f_{(-a)}(\boldsymbol{r}, t)}{\partial r^j \partial r^k}\frac{\partial f_a(\boldsymbol{r}, t)}{\partial r^l} - \frac{\partial f_{(-a)}(\boldsymbol{r}, t)}{\partial r^k}\frac{\partial^2 f_a(\boldsymbol{r}, t)}{\partial r^j \partial r^l}\right) + \cdots\Bigg],\end{aligned} \tag{104}$$

and the part of $\tilde{\boldsymbol{s}}(\boldsymbol{r}, t)$ arising from the quadratic interaction of the wave packets is

$$\tilde{s}^{(2)i}(\boldsymbol{r},t) = -\frac{\hbar}{6} \sum_{aa'a'':\ (-a)\in\mathfrak{A}^{(2)}(a',a'')} \bar{\gamma}^{(2)}_{aa'a''} \Big\{ \omega_a^{(i)} [f_a(\boldsymbol{r},t) f_{a'}(\boldsymbol{r},t) f_{a''}(\boldsymbol{r},t) + f_{a'}(\boldsymbol{r},t) f_a(\boldsymbol{r},t) f_{a''}(\boldsymbol{r},t) + f_{a'}(\boldsymbol{r},t) f_{a''}(\boldsymbol{r},t) f_a(\boldsymbol{r},t)] - i\omega_a^{(ij)} \times \Big[\frac{\partial f_a(\boldsymbol{r},t)}{\partial r^j} f_{a'}(\boldsymbol{r},t) f_{a''}(\boldsymbol{r},t) + f_{a'}(\boldsymbol{r},t) \frac{\partial f_a(\boldsymbol{r},t)}{\partial r^j} f_{a''}(\boldsymbol{r},t) + f_{a'}(\boldsymbol{r},t) f_{a''}(\boldsymbol{r},t) \frac{\partial f_a(\boldsymbol{r},t)}{\partial r^j} \Big] \Big\} \exp(i\Delta^{(2)}_{aa'a''} \cdot \boldsymbol{r}). \quad (105)$$

Both $\tilde{\mathbf{s}}_{0a}(\boldsymbol{r},t)$ and $\tilde{\mathbf{s}}^{(2)}(\boldsymbol{r},t)$ thus defined are Hermitian. We emphasize that with $\tilde{h}(\boldsymbol{r},t)$ and $\tilde{\mathbf{s}}(\boldsymbol{r},t)$ defined by Eqs. (101) and (103), the continuity equation (102) holds exactly. The same is true for the linear quantities $\tilde{h}_{0a}(\boldsymbol{r},t)$ and $\tilde{\mathbf{s}}_{0a}(\boldsymbol{r},t)$ for each wave packet. This means that the effective Poynting vector constituents (104) and (105) exactly match our truncated definition of the effective energy density constituents (90) and (93), although Eq. (103) is not simply an expansion of $\tilde{\mathbf{s}}(\boldsymbol{r},t)$ to the same level that $\tilde{h}(\boldsymbol{r},t)$ is expanded in Eq. (101). The effective Poynting vector $\tilde{\mathbf{s}}(\boldsymbol{r},t)$ can be interpreted as a flux of the effective energy density $\tilde{h}(\boldsymbol{r},t)$.

In many cases, especially for an (approximate) interpretation of results obtained and expressed in terms of the effective fields, rough approximations for $\tilde{h}(\boldsymbol{r},t)$ and $\tilde{\mathbf{s}}(\boldsymbol{r},t)$ suffice,

$$\tilde{h}(\boldsymbol{r},t) \approx \sum_a \frac{\hbar|\omega_a|}{2} f_{(-a)}(\boldsymbol{r},t) f_a(\boldsymbol{r},t) = \sum_{a>0} \hbar\omega_a |g_a(\boldsymbol{r},t)|^2, \quad (106)$$

$$\tilde{\mathbf{s}}(\boldsymbol{r},t) \approx \sum_a \boldsymbol{v}_a \frac{\hbar\omega_a}{2} f_{(-a)}(\boldsymbol{r},t) f_a(\boldsymbol{r},t) = \sum_{a>0} \boldsymbol{v}_a \hbar\omega_a |g_a(\boldsymbol{r},t)|^2, \quad (107)$$

where the expressions with $g_a(\boldsymbol{r},t)$ are given for the classical case. These two formulas provide us with clear additive expressions allowing us to separate contributions from different wave packets. Recall that $v_a^i \equiv \omega_a^{(i)}$ here is the group-velocity vector of the wave packet a.

IV. EXAMPLES

In this section we discuss two simple examples of optical interactions governed by the quadratic susceptibility.

A. Parametric amplification

We first consider the degenerate parametric amplification of a "weak" wave $\boldsymbol{D}_1(\boldsymbol{r},t)$ in a photonic crystal in the presence of a "strong" wave $\boldsymbol{D}_2(\boldsymbol{r},t)$. The solution is well known [2], but the example serves to compare our work with earlier studies. We write

$$\boldsymbol{D}(\boldsymbol{r},t) = \boldsymbol{D}_1(\boldsymbol{r},t) + \boldsymbol{D}_2(\boldsymbol{r},t) + [\boldsymbol{D}_1(\boldsymbol{r},t)]^\dagger + [\boldsymbol{D}_2(\boldsymbol{r},t)]^\dagger, \quad (108)$$

and only consider the cw regime in the undepleted pump approximation, taking $\boldsymbol{D}_2(\boldsymbol{r},t)$ to be a single mode with fixed amplitude A_2,

$$\boldsymbol{D}_2(\boldsymbol{r},t) = A_2 \boldsymbol{D}_{n_2 k_2}(\boldsymbol{r}) \exp(-2i\omega t). \quad (109)$$

Here we denote the strong-wave frequency as $2\omega \equiv \omega_2 \equiv \omega_{n_2\boldsymbol{k}_2}$ and assume that its wave vector $\boldsymbol{k}_2 \| \hat{\mathbf{z}}$. The corresponding effective field,

$$g_2(r,t) = \frac{A_2}{\sqrt{8\pi^3}} \exp(-2i\omega t), \quad (110)$$

does not have any spatial dependence. For the degenerate parametric amplification in cw regime, the time dependence of the weak wave is as follows:

$$g_1(\mathbf{r},t) = \bar{g}_1(\boldsymbol{r}) \exp(-i\omega t). \quad (111)$$

A comparison of this definition with Eq. (99) shows that we have made the amplitude time-independent by choosing the carrier frequency $\bar{\omega}_1 = \omega$. For simplicity, we have assumed that the weak wave is confined to exactly one photonic band n_1. The central wave vector $\boldsymbol{k}_1$ of the weak-wave envelope function is defined below.

The propagation equation for the weak-wave envelope function $\bar{g}_1(\boldsymbol{r})$ is obtained from Eq. (100),

$$\boldsymbol{v}_1 \cdot \frac{\partial \bar{g}_1(\boldsymbol{r})}{\partial \boldsymbol{r}} = -i(\omega_1 - \omega)\bar{g}_1(\boldsymbol{r}) + \frac{2i\bar{\gamma}^{(2)}}{\sqrt{8\pi^3}} A_2 [\bar{g}_1(\boldsymbol{r})]^\dagger \exp[i(\boldsymbol{k}_2 - 2\boldsymbol{k}_1) \cdot \boldsymbol{r}], \quad (112)$$

where $\omega_1 \equiv \omega_{n_1\boldsymbol{k}_1}$ and $\bar{\gamma}^{(2)} \equiv \bar{\gamma}^{(2)}_{(-1)2(-1)} \equiv \Gamma^{(2)}_{n_1 n_2 n_1}([2\bar{\boldsymbol{k}}], -\bar{\boldsymbol{k}})$, where $\bar{\boldsymbol{k}} \equiv \frac{1}{3}[\boldsymbol{k}_1 + \boldsymbol{k}_2]$. By choosing $\boldsymbol{k}_1 = \frac{1}{2}\boldsymbol{k}_2 = \bar{\boldsymbol{k}}$, which gives us a phase-matched set of $\boldsymbol{k}_a$, we eliminate the exponential function in the last equation. We further restrict ourselves to considering the case of exact frequency-matching, where $2\omega_1 = \omega_2 \equiv 2\omega$. We also assume that the group velocity at the point $\boldsymbol{k}_1$ of the photonic band n_1 is $\boldsymbol{v}_1 \| \hat{\mathbf{z}}$, that could be achieved by aligning one of the symmetry directions in the photonic crystal along $\hat{\mathbf{z}}$. All these assumptions simplify the propagation equation for $\bar{g}_1(\boldsymbol{r})$ to

$$\frac{\partial}{\partial z} \bar{g}_1(\boldsymbol{r}) = i\alpha_0 [\bar{g}_1(\boldsymbol{r})]^\dagger, \quad (113)$$

where

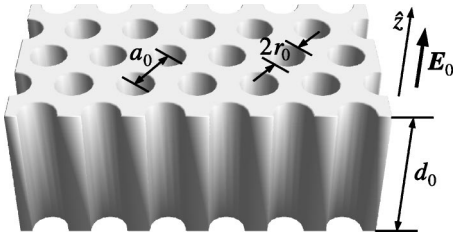

FIG. 4. 2D photonic crystal slab, with holes drilled in a triangular-lattice pattern.

$$\alpha_0 \equiv |\alpha_0| e^{i\phi_0} \equiv \frac{2\overline{\gamma}^{(2)} A_2}{v_1 \sqrt{8\pi^3}}. \tag{114}$$

If we set a boundary condition for the amplitude of the weak wave at $z=0$,

$$\overline{g_1}(z=0) = \overline{g}_{1,0} = \text{const}, \tag{115}$$

we find that $\overline{g_1}(\boldsymbol{r})$ will only depend on z, $\overline{g_1}(\boldsymbol{r}) = \overline{g_1}(z)$, and the solution of Eq. (113) will be as follows:

$$\overline{g_1}(z) = \overline{g}_{1,0} \cosh(|\alpha_0| z) + i e^{i\phi_0} (\overline{g}_{1,0})^{\dagger} \sinh(|\alpha_0| z). \tag{116}$$

Our result agrees with the known solution [2] if we neglect all the differences that are of higher-order than the results themselves. In [2] an *ad hoc* perturbative method was used for obtaining the coordinate dependence of the parametrically amplified signal. This method relies on plane waves, that are functions of the three spatial coordinates, but still uses the propagation length as an extra parameter. While sufficient for illustrating the physical processes behind the parametric amplification in photonic crystals in a plane-wave approximation, the method of [2] is very inconvenient for describing spatially-confined wave packets. On the other hand, the effective-field formalism that we used here makes the description of nonlinear wave-packet interactions in photonic crystals almost as simple as in homogeneous media.

B. Electro-optic effect

Another interesting example of the second-order nonlinear interaction of wave packets is the electro-optic effect, where one of the participating wave packets is in fact a constant electric field—or an electric field oscillating with a very low frequency compared to the optical frequencies—whose amplitude is generally position-dependent. This kind of nonlinear optical interaction is always phase-matched, so the calculations are simpler and employ fewer approximations than in more general scenarios.

As a practical example, we consider a 2D GaAs photonic crystal, where holes of radius r_0 are drilled in a triangular-lattice pattern with the period a_0 (Fig. 4). The sample is of a finite thickness d_0 in the direction of the holes axes, where $d_0 \gg a_0$ is large enough that we can still consider the sample and its photonic bands in the approximation of an infinitely thick 2D photonic crystal. In the simplest case that we describe below, the constant electric field applied to the sample is directed along the hole axes, having a homogeneous field strength E_0. A straightforward generalization of the problem could describe the electric field oscillating with a low frequency that is much smaller than the spectral width of the optical field. A description of an inhomogeneous external electric field may require including longitudinally polarized as well as transverse solutions of the wave equation; this can easily be done in a way similar to the introduction of the transverse modes in this paper. In most practical cases, the inhomogeneous electric field will be a slowly varying function of the spatial coordinates on the scale of the photonic-crystal period a_0.

As in our last example, the total electric field in the electro-optic problem consists of two wave packets and their respective conjugates. One wave packet is an optical field described by the effective field $g_1(\boldsymbol{r},t)$; it has the central wave-vector $\boldsymbol{k}_1$ and the central frequency $\omega_1 \equiv \omega_{n_1 \boldsymbol{k}_1}$. The other wave packet is the zero-frequency electric field with a homogeneous field strength, that is,

$$\boldsymbol{D}_2(\boldsymbol{r},t) = [\boldsymbol{D}_2(\boldsymbol{r},t)]^* = \hat{\mathbf{z}} \varepsilon_0 n^2(\boldsymbol{r}) \frac{E_0}{2}, \tag{117}$$

where $\hat{\mathbf{z}}$ is the unit vector directed along the hole axes, and E_0 is assumed to be real. The field $\boldsymbol{D}_2(\boldsymbol{r},t)$ is proportional to the z-polarized zero-frequency eigenmode,

$$\boldsymbol{d}_{n_2 0}(\boldsymbol{r}) = \hat{\mathbf{z}} \mathcal{N}_2^{-1} \varepsilon_0 n^2(\boldsymbol{r}), \tag{118}$$

where n_2 labels the lowest band. With the normalization that we imposed in Eq. (30), the mode $\boldsymbol{D}_{n_2 0}(\boldsymbol{r})$ [as well as $\boldsymbol{d}_{n_2 0}(\boldsymbol{r})$] would strictly vanish at zero frequency; a different normalization factor $\mathcal{N}_2$ is warranted for this special case. We need not to identify this factor here, since it cancels in the final result. The effective field for the second wave packet is proportional to E_0,

$$g_2(\boldsymbol{r},t) = \mathcal{N}_2 \frac{E_0}{2}, \tag{119}$$

so that, in our particular case,

$$\boldsymbol{D}_2(\boldsymbol{r},t) = g_2(\boldsymbol{r},t) \boldsymbol{d}_{n_2 0}(\boldsymbol{r}). \tag{120}$$

Since E_0 is the fixed external driving field, we only have one equation of motion, that follows from Eq. (98):

$$\frac{\partial}{\partial t} g_1(\boldsymbol{r},t) = -i\omega_1 g_1(\boldsymbol{r},t) - \omega_1^{(i)} \frac{\partial g_1(\boldsymbol{r},t)}{\partial r^i} + \frac{i}{2} \omega_1^{(ij)} \frac{\partial^2 g_1(\boldsymbol{r},t)}{\partial r^i \partial r^j} + \cdots + 2i(\mathcal{N}_2 \overline{\gamma}^{(2)}_{(-1)12}) g_1(\boldsymbol{r},t) E_0. \tag{121}$$

From this equation, we conclude that the introduction of the homogeneous electric field E_0 effectively amounts to a correction

$$\Delta\omega_{\text{eo}} = -2(\mathcal{N}_2 \overline{\gamma}^{(2)}_{(-1)12}) E_0 \tag{122}$$

to the photonic-band frequency ω_1. Figure 5 illustrates the electro-optic frequency shift $\Delta\omega_{\text{eo}}$ for the 1st and 4th TE-polarized modes [that is, the modes with $\boldsymbol{d}_{n_1 \boldsymbol{k}_1}(\boldsymbol{r}) \perp \hat{\mathbf{z}}$; bands are numbered in order of frequencies] in the 2D sample with a triangular lattice of holes; for these bands no degeneracy concerns arise away from the Γ point. In areas of the first Brillouin zone with positive values of $\Delta\omega_{\text{eo}}$ we use solid

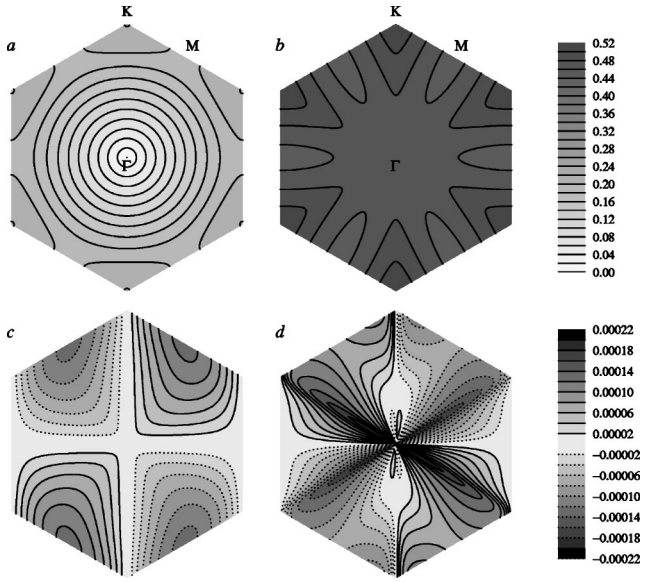

FIG. 5. Normalized frequencies $\omega_1 a_0/c$ [(a), (b)] and the respective electro-optic band-frequency shifts $\Delta\omega_{\mathrm{eo}}$ [(c), (d)] of the 1st [(a), (c)] and 4th [(b), (d)] TE photonic bands plotted vs $\boldsymbol{k}_1$ in the first Brillouin zone of a 2D photonic crystal with a triangular lattice of holes drilled in a GaAs sample.

contour lines, while for negative $\Delta\omega_{\mathrm{eo}}$ we use dotted contour lines. The refractive index of GaAs was taken to be 11.4, which approximately corresponds to the vacuum wavelength $\lambda=1.5$ μm, and the relative hole radius $r_0/a_0=0.332$ that corresponds to the "air-fill factor" of 40%. We taken $\chi^{(2)}_{xyz}E_0=0.01$ and used the relation (7) to express Γ_2^{ijl} in terms of $\underline{\chi}^{(2)}_{ijl}$. In GaAs, which has the *zincblende* lattice structure and 43*m* point symmetry group, both tensors have 6 equal nonzero Cartesian components that are obtained from $\chi^{(2)}_{xyz}$ and Γ_2^{xyz} using all permutations of the tensor indices. One of the crystallographic axes of GaAs is directed along $\hat{\boldsymbol{z}}$, two others are aligned with the ΓK and ΓM directions of the photonic crystal lattice. The effective quadratic susceptibility $\overline{\gamma}^{(2)}_{(-1)12}$, which is responsible for the electro-optic interaction, is expressed in a straightforward manner in terms of the photonic modes and the quadratic susceptibility $\Gamma^{(2)}_{nn'n''}(\boldsymbol{r})$ using Eqs. (94), (73), (48), and (118):

$$\mathcal{N}_2\overline{\gamma}^{(2)}_{(-1)12}=\frac{1}{\hbar\varepsilon_0}\int_{V_{\mathrm{cell}}}\frac{d\boldsymbol{r}}{V_{\mathrm{cell}}}\Gamma_2^{izj}(\boldsymbol{r})[d^i_{n_1\boldsymbol{k}_1}(\boldsymbol{r})]^*\varepsilon_0 n^2(\boldsymbol{r})d^j_{n_1\boldsymbol{k}_1}(\boldsymbol{r}). \tag{123}$$

We computed this integral numerically, with the photonic modes obtained using the MIT Photonic-Bands package [11]. Note that Eq. (121) and (123) can be easily generalized to include the dispersion ($\boldsymbol{k}$-dependence) of $\gamma^{(2)}_{(-1)12}$. The resulting formulas are much simpler if written in the reciprocal space.

The symmetry of the photonic modes in the first Brillouin zone is determined by the symmetry group of the photonic-crystal lattice, since the dielectric tensor of GaAs is isotropic. Applying the electric field lowers the symmetry of GaAs, inducing optical birefringence, so the plots of $\Delta\omega_{\mathrm{eo}}$ in Fig. 5 exhibit lower symmetry than the symmetry of the modes.

The approach to calculating $\Delta\omega_{\mathrm{eo}}$ according to Eqs. (122) and (123) may be described as a perturbative method, where we find the frequency change using a fixed basis set of photonic modes, and $\chi^{(2)}_{izj}E_0$ is the small parameter. Indeed, if we take a small variation of Eq. (35) that arises from changing $\varepsilon_{ij}=n^2\delta_{ij}$ by $2\chi^{(2)}_{izj}E_0$, then use Eqs. (22) and (23), and finally integrate by $\boldsymbol{k}'$ over the first Brillouin zone and sum over n', we will get an expression for $\Delta\omega_{\mathrm{eo}}$, equivalent to Eqs. (122) and (123). As it is common in the perturbation theory, the variation in the modes $(\boldsymbol{D}_{n\boldsymbol{k}}(\boldsymbol{r}),\boldsymbol{B}_{n\boldsymbol{k}}(\boldsymbol{r}))$ does not affect $\omega_{n\boldsymbol{k}}$ in the first approximation, that is, we will have the same $\Delta\omega_{\mathrm{eo}}$, whether we fix the modes, when varying ε_{ij}, or not. Technically, this results because the change in $\omega_{n\boldsymbol{k}}$ arising from the variation in $\boldsymbol{D}_{n\boldsymbol{k}}(\boldsymbol{r})$ in Eq. (35) is equal in the absolute value but opposite in direction to the change arising from the variation in $\boldsymbol{B}_{n\boldsymbol{k}}(\boldsymbol{r})$.

We can also find $\Delta\omega_{\mathrm{eo}}$ by calculating the shift of the photonic band frequencies, arising when we change the dielectric tensor of GaAs $\varepsilon_{ij}=n^2\delta_{ij}$ by an electric-filed induced tensor $2\chi^{(2)}_{izj}E_0$ [cf. Eq. (6)]. The change in the dielectric tensor leads to a change in the photonic band structure, and we compute the difference between the mode frequencies of the modified and original band structures. We have shown by numerical calculations that for small electric fields ($\chi^{(2)}_{izj}E_0 \ll 1$) the frequency shift is very close to the shift computed according to Eqs. (122) and (123); the difference only becomes significant at $\chi^{(2)}_{izj}E_0 \gtrsim 0.1$.

We note, however, that the method of computing $\Delta\omega_{\mathrm{eo}}$ by treating the electro-optic effect as a quadratic nonlinear interaction, as outlined in Eqs. (122) and (123), is much more powerful, since it can be easily generalized to an inhomogeneous distribution of the external electric field. This is important to properly describe controlling of light in photonic crystals with a localized electric field, which has possible applications in building photonic devices. We defer investigation of such more complex examples to a later publication.

Finally, we give some estimates of the electro-optic frequency shift in GaAs. The electro-optic coefficient of GaAs, $r\approx 1.5\times 10^{-12}$ m/V [17], is connected with the quadratic susceptibility tensor used in this paper as $2\chi^{(2)}_{xyz}=\varepsilon^2 r$; the electric field applied to the sample cannot exceed the electric-breakdown threshold of the air, $E^{\mathrm{air}}_{\mathrm{max}}\approx 3\times 10^6$ V/m, which is more than an order of magnitude less than the electric-breakdown threshold of GaAs. This means that the highest achievable value of $\chi^{(2)}_{izj}E_0$ is of the order of 3×10^{-4}, which is in the range where our first-order perturbation approach for $\Delta\omega_{\mathrm{eo}}$ works well. Since $\Delta\omega_{\mathrm{eo}}$ scales linearly with E_0, we can estimate from Fig. 5 that the maximum relative change in the photonic band frequencies $\Delta\omega_{\mathrm{eo}}/\omega_{n\boldsymbol{k}}$ that corresponds to the highest achievable electric field is of the order of 3×10^{-5}. Such small changes in the photonic band frequencies can only be realistically detected at the band edge, as was done recently in a four-wave mixing process [16]. Even in that case and with the constant electric field close to $E^{\mathrm{air}}_{\mathrm{max}}$, such measurements would be at the limit of experimental techniques. To enhance the effect, one could use a material with larger electro-optic coefficient. Another

approach would be to fill the holes of the photonic crystal with a low-index material with much higher electric-breakdown threshold than that of the air, and apply a stronger electric field.

V. CONCLUSION

Using an effective-fields approach introduced earlier for single-wave-packet configuration [6], we have generalized this useful and convenient formalism to describe nonlinear interactions of multiple wave packets. This generalization is not quite straightforward, and involves a modification to the previously used definition of the wave packet itself [6] by introducing the filter functions $\Pi_a(\boldsymbol{\kappa})$, which allows for multiple wave packets within the same photonic band. While this change in the definition of the effective fields leads to a more complicated form of the Poisson bracket that is no longer canonical, this turns out not to be a significant complication for the derivation of the dynamical equations and their use.

In the course of our analysis we have introduced the effective energy density and the effective Poynting vector, which constitute a natural way to describe the average energy distribution and flux of the electromagnetic field in this formalism. The continuity equation that these new quantities satisfy allows for a convenient way of checking the consistency and precision of numerical computations based on the dynamical equations for the effective fields.

In the formulas presented in this paper, we have only retained terms involving the quadratic optical susceptibility. Still, the extension of our theoretical approach to higher-order susceptibilities is very straightforward. The examples of nonlinear optical interactions of wave packets we presented here are deliberately chosen as simple as possible to illustrate the way the formalism works and how it can be used; more complex problems will become subjects of separate papers.

ACKNOWLEDGMENTS

This work was supported by the National Sciences and Engineering Research Council of Canada and Photonics Research Ontario. We are grateful to N. A. R. Bhat for useful discussions.

[1] J. D. Joannopoulos, R. D. Meade, and J. N. Winn, *Photonic Crystals: Molding the Flow of Light* (Princeton University Press, Princeton, NJ, 1995).
[2] K. Sakoda, *Optical Properties of Photonic Crystals* (Springer-Verlag, Berlin-Heidelberg-New York, 2001).
[3] C. M. de Sterke and J. E. Sipe, in *Progress in Optics*, edited by E. Wolf (North-Holland, Amsterdam, 1994), Vol. 33, p. 203.
[4] C. M. de Sterke, D. G. Salinas, and J. E. Sipe, Phys. Rev. E **54**, 1969 (1996).
[5] S. Pereira and J. E. Sipe, Phys. Rev. E **65**, 046601 (2002).
[6] J. E. Sipe, N. A. R. Bhat, P. Chak, and S. Pereira, Phys. Rev. E **69**, 016604 (2004).
[7] See a discussion in Sec. IV of [6].
[8] M. Born and L. Infeld, Proc. R. Soc. London **147**, 522 (1934).
[9] I. Białynicki-Birula and Z. Białynicka-Birula, *Quantum Electrodynamics* (Pergamon, Oxford-New York, 1975).
[10] A. Lukš and V. Peřinová, in *Progress in Optics*, edited by E. Wolf (North-Holland, Amsterdam, 2002), Vol. 43, p. 295.
[11] S. G. Johnson and J. D. Joannopoulos, Opt. Express **8**, 173 (2001).
[12] N. Bloembergen, *Nonlinear Optics* (Plenum, New York, 1969).
[13] R. W. Boyd, *Nonlinear Optics* (Academic, San Diego, 2002).
[14] J. E. Sipe, Phys. Rev. E **62**, 5672 (2000).
[15] N. A. R. Bhat and J. E. Sipe, Phys. Rev. E **64**, 056604 (2001).
[16] H. W. Tan, H. M. van Driel, S. L. Schweizer, R. B. Wehrspohn, and U. Gösele (private communication).
[17] S. S. Lee, R. V. Ramaswamy, and V. S. Sundaram, IEEE J. Quantum Electron. **27**, 726 (1991).